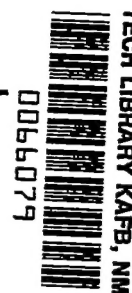# NATIONAL ADVISORY COMMITTEE FOR AERONAUTICS

TECHNICAL NOTE 3190

FATIGUE INVESTIGATION OF FULL-SCALE

TRANSPORT-AIRPLANE WINGS

SUMMARY OF CONSTANT-AMPLITUDE TESTS THROUGH 1953

By M. J. McGuigan, Jr., D. F. Bryan, and R. E. Whaley

Langley Aeronautical Laboratory
Langley Field, Va.

NACA

NATIONAL ADVISORY COMMITTEE FOR AERONAUTICS

TECHNICAL NOTE 3190

FATIGUE INVESTIGATION OF FULL-SCALE

TRANSPORT-AIRPLANE WINGS

SUMMARY OF CONSTANT-AMPLITUDE TESTS THROUGH 1953

By M. J. McGuigan, Jr., D. F. Bryan, and R. E. Whaley

SUMMARY

Results are presented of a fatigue investigation conducted on the wings of C-46 "Commando" airplanes. Constant-amplitude tests were conducted by the resonant-frequency method at four different alternating load levels about a 1 g or level-flight mean load.

All fatigue failures were classified according to the type of structural stress raisers in which they originated. Effective stress-concentration factors were determined for all failures and were found to vary with the load level. The scatter in fatigue life was analyzed statistically and found to be comparable to the scatter obtained in tests of small specimens of the same type of material as that from which the wing was constructed.

Fatigue-crack propagation was investigated and it was found that all cracks grew slowly until a certain critical percentage of the structure had failed, after which the cracks grew rapidly. This critical percentage was found to vary inversely with the load level. The load-lifetime relationship of the test structure was established and found to compare favorably with that of several other full-scale structures which have been subjected to fatigue tests.

Two appendixes are included which present information on the use of bonded wires to detect small fatigue cracks and the use of fiber glass as a method of structural repair.

INTRODUCTION

Few fatigue tests have been conducted on actual airplane structures, and most of the tests that have been accomplished were directed at the solution of some particular problem. In view of the general lack of information regarding the fatigue characteristics of complete airplane

structures, twenty-one C-46 "Commando" airplanes were secured for the pur-
pose of carrying out a fatigue investigation of full-scale airplane wings.
The objectives of the program were to include the determination of the
following: (1) the scatter in fatigue life between structures fabricated
in an identical manner, (2) the relative magnitudes of stress concentra-
tion caused by various types of stress raisers existing in aircraft struc-
tures, (3) the rate and manner of fatigue-crack propagation, (4) the
reduction in static strength after fatigue failure, and (5) the loss in
fatigue life associated with the flight history which an airplane has
experienced. These objectives were to be fulfilled by conducting, on
the C-46 wings, a number of constant-level tests at each of several dif-
ferent load levels and a series of variable-amplitude tests, based on
gust-frequency data, to simulate actual flight loadings.

This report supersedes reference 1 and presents the results of
constant-level tests of eight complete wings conducted at four different
alternating-load levels. The results of these tests provide information
on the first three listed objectives. Included in this report are the
data presented in reference 1 which covered tests at one load level, all
subsequent data at other test levels, and a summary of all information
and conclusions to date for the program. The basic information is sum-
marized in tabular form and derived data such as scatter in lifetime,
effective stress-concentration factors, load-lifetime relationships,
and information on fatigue-crack propagation are included. Appendix A,
which deals with the use of bonded wires to detect fatigue cracks, and
appendix B, which deals with the use of laminated fiber glass for struc-
tural repair, are included because of interest expressed in these subjects.

SPECIMENS AND PROCEDURE

C-46 Structure

The C-46 wings used in these tests had previously been subjected
to from 200 to 940 hours of flight service and storage for several years
in an open depot.

The wing was of all-metal, riveted, stressed-skin construction and
was made almost entirely of 24S-T clad material. The complete wing con-
sisted of a center section and two outer panels. Some of the details
of construction are given in reference 1, and typical cross sections of
the structure are shown in figure 1.

Some geometric characteristics of the wings as well as other perti-
nent data for the C-46 airplane are given in the following table:

Maximum design gross weight, lb 45,000
Design level-flight equivalent airspeed, mph 240
Wing area, sq ft 1,360
Wing span, ft 108
Mean aerodynamic chord, in. 164.25
Aspect ratio 8.58
Thickness at center section, percent chord 17
Design ultimate load factor 4.63

In testing the first few specimens it was found that, under the test
loading, failures sometimes occurred in the center panel of the wing.
Such failure caused cessation of the test before complete information
was obtained from the failures occurring in the outer panels, which were
the components of principal interest. In order to retard these center-
section failures, a reinforcing strip was riveted to the wing skin along
the full span of the center section in all specimens subsequent to those
reported in reference 1. The location and size of this strip are shown
in figure 1. Strain-gage measurements, made to determine the effective-
ness of the reinforcement, indicated that the stresses were reduced only
in the immediate vicinity of the strip, which was the desired effect.
No measurable change was observed in the magnitude or distribution of
the stresses in the outer wing panels.

Instrumentation

In order to obtain information on the stresses present in the struc-
ture where fatigue failures occurred, the wings were instrumented with
a number of wire resistance strain gages with suitable indicating equip-
ment for both static and dynamic measurements. Most of these gages were
located so as to measure the nominal stress near the points where fatigue
failures originated on previous specimens. Other strain gages were used
to determine stress distributions in the wing. A detailed description
of the instrumentation is included in reference 1.

In order to increase the probability of early detection of fatigue
cracks and to reduce the time spent in visual inspection, a fatigue-crack
detection system was used. This system of detection utilized small copper
wires cemented to the wing in the vicinity of stress raisers where fatigue
failures were likely to occur. When a crack occurred and passed under
a wire, the wire broke and an alarm system was actuated. A more detailed
description of these detector wires and of tests to determine their sen-
sitivity is included as appendix A. The detector-wire locations, as well
as most of the strain-gage locations, are shown in figure 2.

Tests and Procedure.

The tests were accomplished by the resonant-frequency method, uti-
lizing concentrated masses to reproduce the 1 g stresses at a selected
wing station. Span station 214, measured in inches from the airplane
center line, was selected as the wing station at which to reproduce these
stresses (ref. 1). Concentrated masses, for attachment to the wing, were
then proportioned and located in such a way that the 1 g bending moment,
shear, and torque at span station 214 were closely reproduced for the
level-flight, low-angle-of-attack condition. Actually, the bending
moment was rather closely reproduced not only at span station 214 but
also over a considerable portion of the span, as can be seen in figure 3.

A specimen is shown mounted and ready for test in figure 4. A
detailed description of the fatigue machine and the preparation of the
specimens for testing is included in reference 1.

The tests were carried out by vibrating the wings at their funda-
mental bending frequency of 108 cycles per minute with the fatigue machine
previously mentioned. Frequent visual inspections of the wings through-
out the tests supplemented the indications from the fatigue-crack detector
wires. Chordwise stress-distribution surveys were made on several of
the wings. At various times throughout the tests, the output of all
strain gages was recorded to check for uniformity of loading. In addi-
tion, damping tests were made periodically during the testing of several
specimens.

Tests have been conducted at four different alternating load levels.
These alternating load levels were 22, 14, 9 and $7\frac{1}{2}$ percent of the design
ultimate load factor, which correspond to airplane incremental load fac-
tors Δn of 1.0, 0.625, 0.425, and 0.35, respectively. The design ulti-
mate load factor was based on the gust requirement. Two complete wings
were tested at the highest level, three at the next highest, two at the
next, and one at the lowest. All tests were conducted with a 1 g or
level-flight mean load given by the concentrated masses attached to the
wing.

The testing of a specimen was continued until a fatigue failure
occurred, at which time the number of load cycles applied was noted.
For purposes of this investigation, initial fatigue failure is defined
as a break in the material of the wing that is approximately $\frac{1}{4}$ inch
long and as deep as the material in which it originated. If the fail-
ure occurred in the wing center section it was usually repaired in order
to continue the testing of the outer panels. The method used for these
repairs is described in appendix B. When a failure occurred in the outer
panel it was allowed to grow and the rate and manner of crack propaga-
tion was noted. Although none of the fatigue tests was continued to

complete or final failure of the wing, the number of cycles to final
failure was estimated from the crack-propagation curves.

RESULTS AND DISCUSSION

Classification and Description of Failures

All the failures that were observed are listed in table 1. For
identification purposes the failures are numbered in order of their
occurrence at each test level. All failures were classified according
to their origin, as follows:

Type I	Corners of inspection cutouts
Type II	Riveted tension joints
Type III	Riveted shear joints
Type IV	Inspection-cutout reinforcements
Type V	Miscellaneous discontinuities

The five types and their locations are shown in the plan view of the
tension surface in figure 5, and are illustrated in figures 6 and 7.
Most of these types of failures occurred in stress raisers which would
be present in similar form on almost any metal aircraft structure.

The type I failures originated in the corners of inspection cut-
outs B, F, G, and H, and examples are shown in figures 6(a) and 6(b).
These cutouts had non-load-carrying covers and were all at span sta-
tion 214. Most of the failures occurred in the vicinity of the spar at
the 30-percent-chord position, which was the most highly stressed region
as indicated by the chordwise stress-distribution survey at this station.
Since span station 214 contained numerous cutouts, doublers, and other
discontinuities and therefore yielded an irregular stress distribution,
another chordwise survey was made at span station 235, which was the
nearest station that was free of these discontinuities. The gages used
in these surveys were oriented so as to measure the strain in a spanwise
direction. The results of these surveys are presented in figure 8, along
with a cross section of the tension surface at span station 214. This
figure indicates that for both of these stations the highest stress occurs
in the vicinity of the 30-percent spar.

The type II failures, which originated in riveted tension joints,
all occurred at span station 32 inside the fuselage in the vicinity of
the 30-percent spar. A photograph of this type of failure is shown as
figure 6(c). A chordwise distribution of stress at span station 32 was
included in reference 1 and indicated that the higher stresses again
occurred in the vicinity of the 30-percent spar. These failures were
consistent during the earlier tests but did not occur during the later
tests because of the reinforcing strip previously described.

The type III failures occurred at span station 120 in the riveted joint connecting the shear web to the tension flange of the front spar. Since this location was very difficult to photograph, a drawing of the details of this joint is shown in figure 7. The cracks usually progressed vertically through the shear web and were accompanied by a crack in a small piece of skin over the spar cap.

The type IV failures occurred in internal reinforcing doubler plates around cutouts D and E, located outboard of span station 214 and immediately forward of the 30-percent spar. A photograph of this type of failure is presented as figure 6(d). These cutouts had cover plates that were fastened to the reinforcing doubler plate with machine screws and channel nuts. The failures originated in the screw holes on some wings and in the smaller-radius corner of the internal doubler plate on others, frequently occurring very early in a test. These failures spread into the skin on only two occasions but in no case did they grow to more than a few inches in length.

Type V includes all the failures that could not be classified in one of the preceeding types. Several failure locations are included in this type, but at only three of these did failures repeatedly occur. One of these locations was in a joggle in an external doubler plate about 3 inches outboard of the wing attach angle and directly over the 30-percent spar. These failures occurred only at the two highest load levels and an example is presented in figure 6(e). Another type V failure occurred in the skin at the edge of the external attach-angle doubler plate, between the 30-percent spar and cutout B. A photograph of this failure location is presented as figure 6(f). Strain-gage measurements indicated this region to have a higher nominal stress than any other location where strain-gage measurements were made. These failures occurred at every test level. Another failure location of type V was inside the engine nacelles at span station 180 in a doubler plate over the front spar. A notch had been cut in the edge of the doubler plate to allow clearance for the rotation of the landing-gear strut during extension and retraction of the landing gear, and the failures started either in the notch or at a rivet near the notch. In some cases the notch had been hand cut and in others the notch was cut by rotation of the landing-gear strut itself. A photograph of this failure is presented as figure 6(g).

Consideration of all the failures that were observed in locations not affected by the center-section reinforcement indicates that failures occurred in a greater number of locations as the load level was increased. This situation is consistent with observations made in some fatigue tests of small specimens, particularly rotating beams, in which more small cracks occurred, other than the one which caused specimen failure, as the stress level was increased (ref. 2).

Scatter in Fatigue Life

From table 1 it can be seen that at any alternating load level there is considerable scatter in the fatigue life. When the lifetime data for initial failure given in table 1 were considered statistically and plotted in the form of probability curves it was found that the probability of failure or survival at any load level was in reasonably good agreement with the statistical theory of extreme values given in reference 3. There are, however, some differences in the manner in which the full-scale fatigue data for the C-46 and the small-specimen data of reference 3 were obtained. Each small specimen yielded one data point, whereas failures occurred at several locations on each of the full-scale specimens. However, failures did not occur at all of these locations on each full-scale specimen. On some of the C-46 wings a failure could not occur at one location because the growth of a failure at another location caused the test to be discontinued. The probability curves drawn for the C-46 were therefore considered to indicate the probability that any failure would occur on the test wings regardless of location.

From the probability curves, data were obtained with which to plot the load-lifetime diagram of figure 9, in which a scatter band is shown. This scatter band indicates the limits within which 95 percent of all failures should occur at each level, as determined by the theory of extreme values. Also shown in this figure are the actual data points obtained from the fatigue tests.

The scatter in fatigue life for all failures that occurred in these tests was comparable to the scatter that has been obtained in tests of small specimens of the same material (ref. 4). In addition, these data indicate no significant trends in scatter with the load level.

Stress-Concentration Factors

An important factor which must enter into any fatigue-strength consideration of an aircraft structure is the reduction in fatigue strength caused by stress raisers, which are always present. Therefore, the relative magnitude of effective stress-concentration factors or fatigue-strength-reduction factors has been determined for each of the stress raisers where fatigue failures originated on the test wings. At the present time there is no single method that is generally accepted for determining this factor when a mean stress other than zero is present. In view of this fact, the effective stress-concentration factor was determined by three methods. These three methods are as follows:

$$K_{F_1} = \frac{\text{Alternating stress in an unnotched specimen}}{\text{Nominal alternating stress in the test specimen}}$$

<div align="right">(at the same mean stress and lifetime)</div>

$$K_{F_2} = \frac{\text{Maximum stress in an unnotched specimen}}{\text{Nominal maximum stress in the test specimen}}$$

<div align="right">(at the same load ratio and lifetime)</div>

$$K_{F_3} = \frac{\text{Maximum stress in an unnotched specimen}}{\text{Nominal maximum stress in the test specimen}}$$

<div align="right">(at the same mean stress and lifetime)</div>

The basic fatigue data for unnotched specimens were obtained from references 4 and 5. The stresses in the test specimen were measured with wire resistance strain gages, located so as to measure the nominal stress in the vicinity of the stress raisers. The measured mean and alternating stresses, and the concentration factors K_{F_1}, K_{F_2}, and K_{F_3} are listed in table 1. The K_{F_2} definition was used to determine the effective stress-concentration factors in reference 1. It can be seen that considerable variation in the effective stress-concentration factor can exist, depending on the manner in which it is defined. Since a mean stress corresponding to a 1 g loading was used throughout these tests and only the alternating load was changed for each test level, the K_{F_1} definition of the effective stress-concentration factor appears best to fit this type of test.

The range of concentration factor K_{F_1} occurring at each load level for the five types of failures is shown in table 2. It can be noted from this table that the concentration factor tends to decrease with increasing load level. This trend is shown graphically in figure 10 for several locations where failures occurred at more than one load level. The trend is assumed to be caused by the increasing effects of plasticity associated with higher stresses as the load level is increased. Both K_{F_2} and K_{F_3} show the same decreasing trend with increasing load level that K_{F_1} does, but in the case of K_{F_3} the trend is not very apparent because of the lower magnitudes involved.

Crack Propagation

The growth of all fatigue cracks was observed during the course of the tests. In figure 11 the growth of typical failures is plotted for each of the test levels. In order to put all failures on the same comparative basis, the percentage of tension material failed in a cross section of the wing is plotted against the percentage of lifetime to final failure. In this figure it can be noted that all of the curves have the same general shape. In each case the failure grew slowly until a certain percentage of the tension material had failed. At this point, defined as the critical point, the growth of the cracks became very rapid. The percentage of tension material that had failed at the critical point decreased with increasing load level. For the 0.35g level the amount of tension material that had failed at the critical point was about 10 percent; for the 0.425g level, about 9 percent; for the 0.625g level, about 6 percent; and for the 1.0g level, about 2 percent. This critical point occurred at about 95 percent of the lifetime to final failure for all test levels. Tests of all specimens were continued until the critical point had been determined.

The propagation curves for the tests at the higher load levels were smooth and regular while the curves for the lower load levels had a tendency to be somewhat irregular. Stiffeners in the wing caused the crack growth to be temporarily retarded at the lower load levels, whereas the crack growth was not retarded by stiffeners at the higher load levels.

It can be seen from this figure that as much as 25 to 40 percent of the final lifetime remains after the inception of the fatigue failure. This situation might indicate that considerable time would exist in a service airplane of similar construction in which to detect and repair a fatigue crack before the failure reached serious proportions. It should be emphasized, however, that the data presented were obtained from constant-amplitude tests and are not necessarily representative of the propagation of a crack under variable-amplitude service loadings.

Effect of Fatigue Damage on Natural Frequency and Damping

Since these tests were accomplished at the resonant frequency of the test wings and the damping of these wings was very low (ref. 6), the test method itself gave a good indication of the effects of fatigue damage on the natural frequency and damping. Any change in the natural frequency or damping would be indicated by a change in the amplitude of vibration. No such change in amplitude was noted during the course of the tests prior to the development of a fatigue crack. Even after a fatigue crack had originated the natural frequency decreased only 2 percent when as much as 55 percent of the tension material had failed.

An additional investigation was conducted to determine whether the damping characteristics of the test specimens changed during the tests. Damping measurements were obtained from the rate of decay of free vibrations of several specimens periodically during the tests. These measurements showed no appreciable change in the structural damping of the test specimens before the development of fatigue failures or even until the failures were of considerable size.

Measurements of the natural frequency or structural damping characteristics would, therefore, appear to be of no practical value as an indication of incipient fatigue failure.

Fatigue Life

The number of cycles to initial failure is included in table 1. The fatigue life for this structure at the various test levels appeared in figure 9 in the form of a load-lifetime diagram. This figure showed the load-lifetime diagram for initial failure, as previously defined, for all failures that occurred during the tests. For no apparent reason some of these failures never grew to more than an inch in length, while others grew to a considerable size. In figure 12 is shown the load-lifetime diagram of initial and final failure for those failures that grew until their respective crack-propagation curves indicated that the critical percentage of tension material had failed. The number of cycles to final failure, estimated from the individual crack-propagation curves for each of the failures, is listed in table 1. It is evident from the rate of crack growth indicated by the curves of figure 11 that this estimate would not be much in error.

The load-lifetime diagram for final failure is presented in figure 13, along with results of fatigue tests on a number of other airplane structures taken from references 7 to 10. The load is given in percent of the ultimate static strength of the structure. It can be seen from this figure that all of the full-scale data presented lie within a comparatively narrow scatter band, considering the fact that the data include different types of airplanes and components with many types of stress raisers. Full-scale fatigue data from other airplanes have been found to fall within the scatter of the data that are presented.

All the points were corrected to a load ratio of zero by means of constant-lifetime diagrams for unnotched specimens from references 4 and 11. The load ratio R is defined as the ratio of the minimum load to the maximum load in a loading cycle. All corrections were relatively small except for those points corrected from $R = -1$. The Meteor 4 tailplanes were tested at a load ratio of $R = -1$ while the remainder of the structures were tested at $R = 0$ or small positive R values.

Since the ordinate of figure 13 is based on the ultimate strength of the structures and since fatigue failures occurred principally on the tension surface, the load-lifetime comparison could best be made on the basis of the ultimate strength of that surface. In the static tests to determine the ultimate strength of the structures in references 7 to 10, the P-51 wing and Meteor 4 tailplane failed in compression while the remaining structures failed in tension. The C-46 curve in this figure is based on the design ultimate strength of the wing, because the actual ultimate strength is unknown. In static tests performed by the U. S. Air Force the wing failed in compression at 95 percent of the design ultimate load, and was subsequently reinforced but not retested.

If, in the case of those structures which failed in compression, the strength of the tension surface is assumed to be greater than the strength used in the comparison of figure 13, the load-lifetime curves would be shifted downward. This downward shift would very likely result in even less scatter in the data of this figure than is now present.

CONCLUDING REMARKS

Constant-amplitude fatigue tests have been conducted on eight complete C-46 airplane wings at four different alternating load levels, utilizing a mean load of 1 g in all tests. All fatigue failures were classified into five types according to the structural stress raisers in which they originated, and these types were considered to be representative of the stress raisers common to most aircraft structures.

Effective stress-concentration factors, which were calculated by several methods for each of the stress raisers where failures occurred, were found to decrease with increasing load level.

The scatter for all failures at each test level was found to be comparable to the scatter that has been obtained in tests on small specimens of the same material.

Fatigue-crack propagation was investigated and it was found that failures grew slowly until a critical percentage of tension material had failed, after which propagation of the cracks became very rapid. This critical percentage was found to vary inversely with the load level, and occurred at about 95 percent of the lifetime to final failure.

The load-lifetime relationship of the test structure compared favorably with the results of fatigue tests on a number of other full-scale structures. All of the full-scale data that were compared were found to be within a relatively narrow scatter band.

Langley Aeronautical Laboratory,
       National Advisory Committee for Aeronautics,
            Langley Field, Va., February 26, 1954.

APPENDIX A

NOTES ON THE USE OF BONDED WIRES TO DETECT FATIGUE CRACKS

By M. H. Levin

Introduction

In connection with the investigation of the fatigue strength of full-scale airplane wing structures, a need arose for a means of detecting small fatigue cracks. The application of bonded wires appeared to be the most satisfactory solution to the problem. These small wires were cemented to the structure where fatigue failures were likely to occur. When a fatigue crack did occur and passed under the wire, an extremely high strain resulted in the wire over a very small length, causing failure of the wire. By use of an electrical circuit, a break in a detector wire caused by a fatigue crack could actuate a warning system and thus materially reduce the time spent in visual inspection.

The combination of 0.002-inch-diameter annealed copper wire and Duco cement had previously been used to detect fatigue cracks (ref. 12). Other combinations of wires and cements had also been used, but no quantitative information could be found regarding the crack-detection sensitivity of these bonded wires. Because of this lack of information it was decided to investigate some commercially available combinations of wire types, wire sizes, and cements.

Tests and Results

A typical test specimen is shown in figure 14. These test specimens were cut from 0.032-inch-thick 24S-T aluminum-alloy sheet and contained a stress raiser in the form of a drilled hole or notch to localize the area of fatigue-crack formation.

The fatigue-crack detector wire was placed in series with a voltage source and relay. The failure of the wire opened the relay and actuated circuits that interrupted the power to the testing machine. The width of the fatigue crack directly beneath the detector wire was taken to be a measure of the sensitivity of the wire and cement combination. Annealed copper wire was used in most of the tests and the sensitivity of several sizes was determined. Four different bonding agents were tested with one size of the annealed copper wire. These were Duco, Bakelite, and Polymerin cements and Paraplex P-43 compound.

A summary of the results is presented in table 3. It was found that both the 0.002-inch-diameter and 0.0012-inch-diameter Formex insulated annealed copper wire when used with Duco cement detected fatigue cracks after they had attained widths of 0.00022 to 0.00067 inch. These wire and cement combinations proved to be the most sensitive and easiest to apply of the combinations tested; however, the 0.0012-inch-diameter wire failed in some instances without the presence of a crack in the sheet specimen.

Application to a Full-Scale Structure

As a result of the investigation just described, the combination of 0.002-inch-diameter Formex insulated annealed copper wire bonded with Duco cement was used to indicate the presence of small cracks in the fatigue tests of C-46 wings. In many instances it was impossible to detect a fatigue crack with the naked eye after a detector wire had indicated that one was present. In some cases the crack could not be seen even with the aid of a 20-power microscope. After additional cycles of load were applied, however, the crack usually became visible at the location indicated by the wire.

The application of these detector wires to the fatigue tests of full-scale wings required a multiwire installation. One channel of the system used is shown schematically in figure 15. When a fatigue crack caused failure of the detector wire the neon lamp would be extinguished and the Thyratron tube would actuate the alarm circuit. By the use of a four-pole, 360 rpm selector switch, it was possible to provide, in a compact arrangement, dependable fatigue-crack indications for 56 circuits. In the process of working out suitable indicating circuits it was found that the installed annealed copper wires would safely carry currents to 0.2 ampere, and with the added insulation afforded by the Duco cement the working voltage between the wire and the test surface could be as high as 150 volts d.c.

The installation procedures for these wires was very similar to that used in the installation of resistance wire strain gages, and considerable care and cleanliness was required in order to obtain dependable indications.

APPENDIX B

NOTES ON LAMINATED FIBER GLASS FOR STRUCTURAL REPAIR

DURING FATIGUE TESTS ON C-46 WINGS

In fatigue tests of the first few C-46 wings it was found that, under the test loading, fatigue failures occurred not only in the outer panels but also in the center panel of the wing. If these center-panel failures were allowed to propagate unimpeded, complete failure of the center section might result, causing cessation of the test before all the desired information was obtained from the outer panels, which were the components of primary interest. Some type of repair of these center-panel failures in the early stage of their development was therefore necessary. It was found that riveted sheet-metal repairs were unsatisfactory because of the cost and time required. In addition, transfer of load from the wing structure to the sheet-metal patch without considerable stress concentration at the edge of the patch was difficult to obtain. An investigation of other possible methods of structural repair indicated that reinforcement with laminated fiber-glass fabric might prove to be satisfactory. Accordingly, a fiber-glass repair method, suggested by Mr. R. E. Little and developed by Mr. Charles B. King, both of the Langley Aeronautical Laboratory, was utilized, where necessary, on all subsequent wings that were fatigue tested. This method proved to be entirely satisfactory, and reduced the cost and time required for repairs by a considerable amount.

All fatigue cracks which were repaired by this method extended in essentially a chordwise direction on the tension surface of the wing. The patches were therefore designed principally to carry tension loads in a spanwise direction. For these fatigue tests the tension surface of the wing was the upper surface since the wing was mounted in the inverted position. The size of the patch required for satisfactory reinforcement naturally depended to some extent on the size of the fatigue crack to be repaired. The length and width of the reinforcement were determined by a generous estimation of the bond area necessary to secure adequate transfer of load from the wing structure to the fiber-glass reinforcement. Since the modulus of elasticity of the reinforcing material was considerably less than that of the aluminum wing structure, the thickness of reinforcement used was about five times the thickness of the structure to be repaired, so that both had about the same stiffness. All reinforcements were laminated from 10 to 16 layers of fiber-glass cloth arranged in a tapering stack which reached its maximum or design thickness over the fatigue crack. This arrangement is shown schematically in figure 16.

Before applying the fiber-glass reinforcement, all traces of dirt,
oil, grease, and synthetic finish were removed from the area to be
repaired with a suitable solvent, and the area was then sandblasted with
fine lake sand to improve the adhesion of the synthetic laminating resin
to the bare metal.

Glass fabric plies 0.018 inch thick were laminated on the metal
structure, using a blend of unsaturated polyester resins mixed with a
catalyst and accelerator to insure a complete cure of the laminating
resin at room temperature.

A thin coat of laminating resin was applied to the prepared surface
and a tailored ply of glass fabric was placed in position and smoothed
out to eliminate air entrapped beneath the ply and insure that the fabric
conformed to irregular contours such as rivet heads. Additional resin
was used to completely impregnate the fabric ply, and the remaining
layers of fabric were applied and impregnated in sequence in the same
manner. The completed reinforcement was covered with a polyvinyl-
alcohol plastic film, to which the resin would not adhere, so that a
uniform pressure of about 2 to 4 pounds per square inch could be applied
to force out any entrapped air and excess resin. It was found advantageous
to speed up the curing of the polyester resin by heating the laminate to
about 150° F with portable infrared lamps. The average elapsed time
required to accomplish one of these repairs was about 10 hours.

A number of these fiber-glass reinforcements have been used in the
fatigue tests of the C-46 wings to repair structural damage resulting
from fatigue cracks of several different types ranging in length from
1/4 inch to 12 inches. Two typical repairs are shown in figure 17.
Part (a) of this figure shows the repair of a failure in a riveted
tension joint at span station 32 similar to the failure shown in fig-
ure 6(c). Part (b) of figure 17 shows the repair of a failure inside
the engine nacelle similar to the failure shown in figure 6(g). The
latter location illustrates how these fiber-glass reinforcements may be
cut to conform to various structural discontinuities. Repairs have also
been made to the shear web of the front spar in the wing center section
at station 120. In this case the fiber-glass reinforcement was applied
to a vertical surface without great difficulty.

In one case it became necessary to patch a failure in the outer
panel. Failure of the 30-percent spar cap and several inches of skin
was successfully repaired by using thicker laminations of fiber glass on
the skin over the 30-percent spar cap. This wing was then used as a
"dummy" wing to allow more complete crack-propagation information to be
obtained from other outer wing panels.

It is estimated that some of the reinforcements, applied after
failure originated, increased the fatigue life of the wing center section

by a factor greater than 2. Several of the repaired areas were cut from
the structure and examined after completion of the fatigue test. It was
found that in no case had the fatigue crack grown after the reinforcement
had been applied.

In view of the fact that this method of fiber-glass repair has
proved so successful in this application, it appears that this technique
might be applicable to other types of structural testing as well as to
the temporary repair of minor damage in actual service airplanes. In
the latter case it might serve as a quick and economical reinforcement
until such time as permanent repairs or replacements could be made.

REFERENCES

1. McGuigan, M. James, Jr.: Interim Report on a Fatigue Investigation
    of a Full-Scale Transport Aircraft Wing Structure. NACA TN 2920,
    1953.

2. Bennett, J. A.: A Study of the Damaging Effect of Fatigue Stressing
    on X4130 Steel. Proc. A.S.T.M., vol. 46, 1946, pp. 693-711.

3. Freudenthal, A. M., and Gumbel, E. J.: On the Statistical Interpreta-
    tion of Fatigue Tests. Proc. Roy. Soc. (London), ser. A., vol. 216,
    no. 1126, Feb. 10, 1953, pp. 309-332.

4. Russell, H. W., Jackson, L. R., Grover, H. J., and Beaver, W. W.:
    Fatigue Strength and Related Characteristics of Aircraft Joints.
    II - Fatigue Characteristics of Sheet and Riveted Joints of
    0.040-Inch 24S-T, 75S-T, and R303-T275 Aluminum Alloys. NACA
    TN 1485, 1948.

5. Luthander, S., and Wållgren, G.: An Experimental Determination of
    the Fatigue Diagram for Tension and Compression in Alclad Sheet.
    Translation No. 8 (FFA Rep. No. 5), Royal Swedish Air Board
    (Stockholm), 1948.

6. Fearnow, Dwight O.: Investigation of the Structural Damping of a
    Full-Scale Airplane Wing. NACA TN 2594, 1952.

7. Patching, C. A.: Interim Note on Repeated Load Testing of "Mustang"
    P-51D Wings. SM. Note 189, Aero. Res. Labs. (Melbourne), Sept. 1951.

8. Johnstone, W. W., Patching, C. A., and Payne, A. O.: An Experimental
    Determination of the Fatigue Strength of CA-12 "Boomerang" Wings.
    Rep. SM. 160, Aero. Res. Labs. (Melbourne), Sept. 1950.

9. Raithby, K. D.: Fatigue Tests on Typical Two Spar Light Alloy
    Structures (Meteor 4 Tailplanes) Under Reversed Loading.
    Rep. No. Structures 108, British R.A.E., May 1951.

10. Fisher, W. A. P.: A Comparison of the Endurance of Various Aircraft
    Structures Under Fluctuating Loading. Rep. No. Structures 45,
    British R.A.E., July 1949.

11. Grover, H. J., Bishop, S. M., and Jackson, L. R.: Fatigue Strengths
    of Aircraft Materials. Axial-Load Fatigue Tests on Unnotched
    Sheet Specimens of 24S-T3 and 75S-T6 Aluminum Alloys and of
    SAE 4130 Steel. NACA TN 2324, 1951.

12. Foster, Henry W.: A Method of Detecting Incipient Fatigue Failure.
    Proc. Soc. Exp. Stress Analysis, vol. IV, no. 2, 1947, pp. 25-31.

TABLE 1

SUMMARY OF DATA

(a) Δn = 1.000; R = 0

Failure (a)	Location of failure (b)	Type of failure	Measured stress (c)		Cycles to failure	K_{F_1}	K_{F_2}	K_{F_3}	Final failure of wing, cycles
			1 g mean, psi	Alternating, psi					
1	Internal reinforcing doubler plate of inspection cutout E, station 239, (L, OP, 7)	IV	6,000	6,000	38,830	4.73	4.40	2.86	
2	Internal reinforcing doubler plate of inspection cutout E, station 239, (R, OP, 7)	IV	6,000	6,000	39,830	4.46	4.36	2.73	
3	Edge of external doubler plate, station 207, (L, OP, 7)	V	9,640	9,640	82,200	2.28	2.16	1.64	110,000
4	Internal reinforcing doubler plate of inspection cutout D, station 228, (R, OP, 7)	IV	6,260	6,260	60,275	3.88	3.70	2.44	
5	Internal reinforcing doubler plate of inspection cutout D, station 228, (L, OP, 7)	IV	6,260	6,260	76,550	3.61	3.40	2.30	
6	Corner of inspection cutout F, station 214, (R, OP, 7)	I	6,570	6,570	82,500	3.32	3.17	2.14	102,100
7	Joggle in external doubler plate, station 195, (L, OP, 7)	V	4,850	4,850	82,890	4.57	4.29	2.79	
8	Corner of inspection cutout H, station 214, (L, OP, 7)	I	5,210	5,210	91,400	4.15	3.86	2.57	
9	Corner of inspection cutout H, station 214, (R, OP, 7)	I	5,210	5,210	93,760	4.06	3.84	2.53	
10 (4)	Internal reinforcing doubler plate of inspection cutout D, station 228, (R, OP, 8)	IV	6,260	6,260	23,360	5.11	4.65	3.06	
11	Outboard juncture of wing and nacelle, station 180, (L, CS, 8)	V	7,190	7,190	28,560	4.23	3.92	2.62	
12 (6)	Corner of inspection cutout F, station 214, (R, OP, 8)	I	6,570	6,570	42,000	4.08	3.93	2.54	67,000
13	Corner of inspection cutout F, station 214, (L, OP, 8)	I	6,570	6,570	50,500	3.85	3.73	2.43	
14 (5)	Internal reinforcing doubler plate of inspection cutout D, station 228, (L, OP, 8)	IV	6,260	6,260	54,270	3.97	3.82	2.48	
15 (3)	Edge of external doubler plate, station 207, (L, OP, 8)	V	9,640	9,640	56,740	2.57	2.45	1.79	76,700
16 (8)	Corner of inspection cutout H, station 214, (L, OP, 8)	I	5,210	5,210	73,670	4.38	4.13	2.69	

[a] Numbers in parentheses indicate failures that occurred in same location.

[b] Letters in parentheses refer to the following: L, left wing; R, right wing; CS, center section; OP, outer panel. Numbers in parentheses refer to the order in which wing panels were tested.

[c] Nominal stress values near point of failure.

TABLE 1.- Continued

SUMMARY OF DATA

(b) $\Delta n = 0.625$; $R = 0.251$

Failure (a)	Location of failure (b)	Type of failure	Measured stress (c)		Cycles to failure	K_{F_1}	K_{F_2}	K_{F_3}	Final failure of wing, cycles
			1 g mean, psi	Alternating, psi					
1	Riveted tension joint, station 32, (L, CS, 1)	II	11,260	7,040	170,632	2.61	2.33	1.62	
2	Riveted tension joint, station 32, (R, CS, 1)	II	11,210	7,010	195,534	2.54	2.26	1.59	
3	Corner of inspection cutout F, station 214, (R, OP, 1)	I	6,570	4,110	195,534	4.35	3.86	2.29	292,000
4	Joggle in external doubler plate, station 195, (L, OP, 1)	V	4,850	3,030	204,448	5.83	5.18	2.86	383,000
5	Corner of inspection cutout H, station 214, (L, OP, 1)	I	5,210	3,260	282,701	5.10	4.46	2.57	
6	Outboard juncture of wing and nacelle, station 180, (R, CS, 2)	V	6,970	4,350	171,371	4.22	3.76	2.24	
7	Outboard juncture of wing and nacelle, station 180, (L, CS, 2)	V	7,190	4,490	171,371	4.12	3.64	2.20	
8	Riveted shear joint, station 120, (R, CS, 2)	III	8,800	5,500	171,371	3.34	2.98	1.90	
9	Riveted shear joint, station 120, (L, CS, 2)	III	8,800	5,500	171,371	3.34	2.98	1.90	
10	Joggle in external doubler plate, station 189, (L, CS, 2)	V	4,750	2,970	274,369	5.62	4.92	2.78	
11 (1)	Riveted tension joint, station 32, (L, CS, 2)	II	10,130	6,330	308,279	2.57	2.25	1.60	
12	Edge of external doubler plate, station 207, (R, OP, 2)	V	9,640	6,020	227,023	2.87	2.54	1.72	262,000
13	Inboard juncture of wing and nacelle, station 135, (L, CS, 2)	V	6,130	3,830	342,664	4.10	3.64	2.19	
14 (2)	Riveted tension joint, station 32, (R, CS, 2)	II	9,960	6,220	355,071	2.47	2.22	1.57	
15	Edge of external doubler plate, station 207, (L, OP, 2)	V	9,640	6,020	285,000	2.76	2.31	1.67	344,000
16 (4)	Joggle in external doubler plate, station 195, (L, OP, 2)	V	4,850	3,030	238,446	5.67	5.00	2.80	
17 (5)	Corner of inspection cutout H, station 214, (L, OP, 2)	I	5,210	3,260	251,799	5.22	4.57	2.62	

a Numbers in parentheses indicate failures that occurred in same location.

b Letters in parentheses refer to the following: L, left wing; R, right wing; CS, center section; OP, outer panel. Numbers in parentheses refer to the order in which wing panels were tested.

c Nominal stress values near point of failure.

TABLE 1.- Continued

SUMMARY OF DATA

(b) $\Delta n = 0.625$; $R = 0.231$ - Concluded

Failure (a)	Location of failure (b)	Type of failure	Measured stress (c)		Cycles to failure	K_{F_1}	K_{F_2}	K_{F_3}	Final failure of wing, cycles
			1 g mean, psi	Alternating, psi					
18 (7)	Outboard juncture of wing and nacelle, station 180, (L, CS, 3)	V	7,190	4,490	78,120	4.94	4.54	2.52	
19 (6)	Outboard juncture of wing and nacelle, station 180, (R, CS, 3)	V	6,970	4,350	119,733	4.48	4.17	2.34	
20 (8)	Riveted shear joint, station 120, (R, CS, 3)	III	8,590	5,370	143,170	3.54	3.21	1.98	
21 (9)	Riveted shear joint, station 120, (L, CS, 3)	III	8,590	5,370	143,170	3.54	3.21	1.98	
22 (2, 14)	Riveted tension joint, station 32, (R, CS, 3)	II	10,950	6,840	164,463	2.72	2.43	1.66	
23 (1, 11)	Riveted tension joint, station 32, (L, CS, 3)	II	10,910	6,820	164,463	2.73	2.44	1.66	
24	Front spar tension flange, station 11, (L, CS, 3)	V	7,730	4,830	217,096	3.62	3.20	2.01	
25	Internal reinforcing doubler plate of inspection cutout D, station 228, (R, OP, 3)	IV	6,260	3,910	245,245	4.40	3.84	2.31	
26	Corner of inspection cutout H, station 214, (R, OP, 3)	I	5,210	3,560	245,245	5.25	4.61	2.63	
27	Internal reinforcing doubler plate of inspection cutout E, station 239, (L, OP, 3)	IV	6,000	3,750	220,072	4.67	4.10	2.41	
28 (8, 20)	Riveted shear joint, station 120, (R, CS, 4)	III	8,330	5,210	93,712	4.00	3.72	2.15	
29	Joggle in external doubler plate, station 195, (R, OP, 3)	V	4,740	2,960	334,598	5.37	4.73	2.68	
30 (7, 18)	Outboard juncture of wing and nacelle, station 180, (L, CS, 4)	V	7,190	4,490	117,541	4.38	4.06	2.30	
31	Corner of inspection cutout B, station 214, (L, OP, 3)	I	6,160	3,850	268,403	4.39	3.83	2.30	342,000
32 (9, 21)	Riveted shear joint, station 120, (L, CS, 4)	III	8,330	5,210	152,650	3.63	3.25	2.01	
33 (5, 17)	Corner of inspection cutout H, station 214, (L, OP, 3)	I	5,210	3,560	298,000	5.03	4.40	2.55	
34	Corner of inspection cutout G, station 206, (L, OP, 3)	I	5,530	3,460	301,469	4.74	4.14	2.44	

[a] Numbers in parentheses indicate failures that occurred in same location.

[b] Letters in parentheses refer to the following: L, left wing; R, right wing; CS, center section; OP, outer panel. Numbers in parentheses refer to the order in which wing panels were tested.

[c] Nominal stress values near point of failure.

TABLE 1.- Continued

SUMMARY OF DATA

(c) $\Delta n = 0.425$; $R = 0.405$

Failure (a)	Location of failure (b)	Type of failure	Measured stress (c)		Cycles to failure	K_{F_1}	K_{F_2}	K_{F_3}	Final failure of wing, cycles
			1 g mean, psi	Alter- nating, psi					
1	Internal reinforcing doubler plate of inspection cutout D, station 228, (L, OP, 4)	IV	6,260	2,660	211,387	6.54	5.60	1.38	
2	Corner of inspection cutout H, station 214, (L, OP, 4)	I	5,210	2,210	602,753	5.96	5.25	2.47	
3	Riveted shear joint, station 120, (L, CS, 5)	III	8,590	3,650	846,937	3.42	2.97	1.73	
4	Internal reinforcing doubler plate of inspection cutout D, station 228, (R, OP, 4)	IV	6,260	2,660	918,469	4.73	4.03	2.11	
5	Edge of external doubler plate, station 207, (L, OP, 4)	V	9,640	4,100	939,200	3.00	2.61	1.60	1,225,000
6	Outboard juncture of wing and nacelle, station 180, (L, CS, 5)	V	7,190	3,060	995,880	4.06	3.46	1.92	
7	Edge of external doubler plate, station 207, (R, OP, 4)	V	9,640	4,100	961,200	3.00	2.60	1.60	1,280,000
8	Corner of inspection cutout H, station 214, (R, OP, 4)	I	5,210	2,210	1,123,647	5.55	4.68	2.37	
9	Corner of inspection cutout B, station 214, (L, OP, 5)	I	6,160	2,620	486,000	5.24	4.65	2.26	1,180,000
10	Corner of inspection cutout B, station 214, (R, OP, 5)	I	6,160	2,620	489,000	5.23	4.64	2.26	
11 (6)	Outboard juncture of wing and nacelle, station 180, (L, CS, 6)	V	7,190	3,060	518,053	4.32	3.93	1.98	
12	Outboard juncture of wing and nacelle, station 180, (R, CS, 6)	V	6,970	2,960	609,190	4.42	3.91	2.02	

[a]Numbers in parentheses indicate failures that occurred in same location.

[b]Letters in parentheses refer to the following: L, left wing; R, right wing; CS, center section; OP, outer panel.
Numbers in parentheses refer to the order in which wing panels were tested.

[c]Nominal stress values near point of failure.

TABLE 1.- Concluded

SUMMARY OF DATA

(d) $\Delta n = 0.350;$ $R = 0.481$

| Failure (a) | Location of failure (b) | Type of failure | Measured stress (c) | | Cycles to failure | K_{F_1} | K_{F_2} | K_{F_3} | Final failure of wing, cycles |
			1 g mean, psi	Alter- nating, psi					
1	Internal reinforcing doubler plate of inspection cutout E, station 239, (L, OP, 6)	IV	6,000	2,100	580,978	6.33	5.45	2.38	
2	Internal reinforcing doubler plate of inspection cutout E, station 239, (R, OP, 6)	IV	6,000	2,100	864,057	6.04	5.03	2.31	
3	Edge of external doubler plate, station 207, (L, OP, 6)	V	9,640	3,370	1,235,581	3.56	2.96	1.66	2,019,000
4	Outboard juncture of wing and nacelle, station 180, (L, CS, 7)	V	7,190	2,520	1,193,000	4.77	4.00	1.98	
5	Edge of external doubler plate, station 207, (R, OP, 6)	V	9,640	3,370	1,060,000	3.58	3.04	1.67	2,000,000

[a]Numbers in parentheses indicate failures that occurred in same location.

[b]Letters in parentheses refer to the following: L, left wing; R, right wing; CS, center section; OP, outer panel.
Numbers in parentheses refer to the order in which wing panels were tested.

[c]Nominal stress values near point of failure.

TABLE 2

STRESS-CONCENTRATION FACTOR K_{F_1}

Test level, Δn	Type I, corner of inspection cutout	Type II, riveted tension joint	Type III, riveted shear joint	Type IV, cutout reinforce- ment	Type V, miscellaneous discon- tinuities
0.350	-----------	-----------	-----------	6.0 to 6.3	3.6 to 4.8
.425	5.2 to 6.0	-----------	3.4	4.7 to 6.5	3.0 to 4.4
.625	4.4 to 5.3	2.5 to 2.7	3.3 to 4.0	4.4 to 4.7	2.8 to 5.8
1.000	3.3 to 4.4	-----------	-----------	3.6 to 5.1	2.3 to 4.6

TABLE 3

RESULTS OF TESTS ON BONDED WIRES USED AS FATIGUE-CRACK INDICATORS

Wire insulation (a)	Nominal wire diameter, in.	Cement	Nominal maximum stress, psi	Cycles to failure	Width of crack detected, in.	Remarks
Formex Type F	0.002	Duco	18,700	281,000	0.00067	Width of crack determined with test specimen under peak tension load
Formex Type F	.002	Duco	26,200	52,500	.00034	Do.
Formex Type F	.002	Duco	25,500	34,900	.00039	Do.
Formex Type F	.002	Duco	28,200	11,800	.00022	Do.
Formex Type HF	.0012	Duco	22,500	9,300	.00035	Do.
Formex Type HF	.0012	Duco	25,500	8,500	.00058	Do.
Formex Type HF	.0012	Duco	9,220	353,000	-------	Wire broke with no crack in specimen
Formex Type HF	.0012	Duco	9,220	543,000	-------	New wire mounted on preceding specimen; wire again broke with no crack in specimen
Formex Type HF	.0012	Duco	18,800	976,500	-------	Wire broke with no crack in specimen
Formex Type HF	.0012	Duco	18,800	166,500	-------	New wire mounted on preceding specimen; wire again broke with no crack in specimen
Formex Type F	.002	Duco	15,100	7,804,700	-------	Test specimen did not fail
Formex Type F	.002	Duco	12,600	10,640,000	-------	Test specimen did not fail
Formex Type F	.002	Polymerin	------	----------	-------	Clamping and baking procedures required for cements caused formation of kinks in wires, cracks in wire insulation, and difficulty in locating wires in desired positions
Formex Type F	.002	Bakelite	------	----------	-------	Do.
Formex Type F	.002	Paraplex P-43	------	2,185,200	.003	Width of crack determined with no load on test specimen
Formex Type F	.002	Paraplex P-43	29,850	2,207,900	-------	Test specimen did not fail
Enamel	.001	Duco	------	392,400	-------	Wire was difficult to handle and was easily kinked; insulation was easily cracked
None[b]	.0015	Duco	29,850	109,800	.004	Width of crack determined with no load on test specimen

[a]Wire material was annealed copper unless otherwise stated.

[b]Wire material was a copper-nickel alloy.

30-percent-chord spar

70-percent-chord spar

Front spar

Center-panel structure

3/16

$2\frac{5}{8}$

$3\frac{5}{8}$

Details of reinforcement strip

Hat-section stiffeners

Outer-panel structure
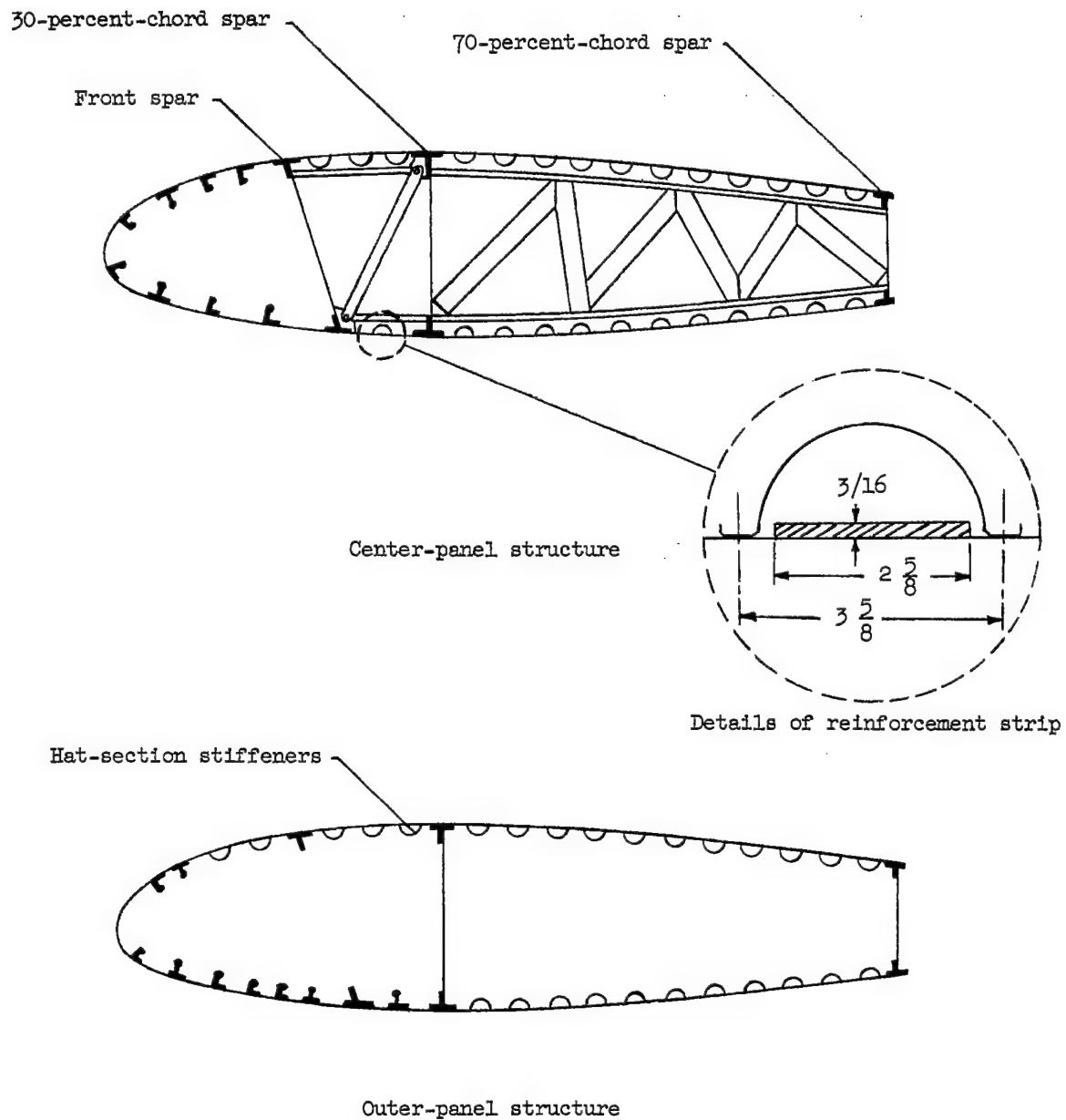
Figure 1.- Typical sections of wing.
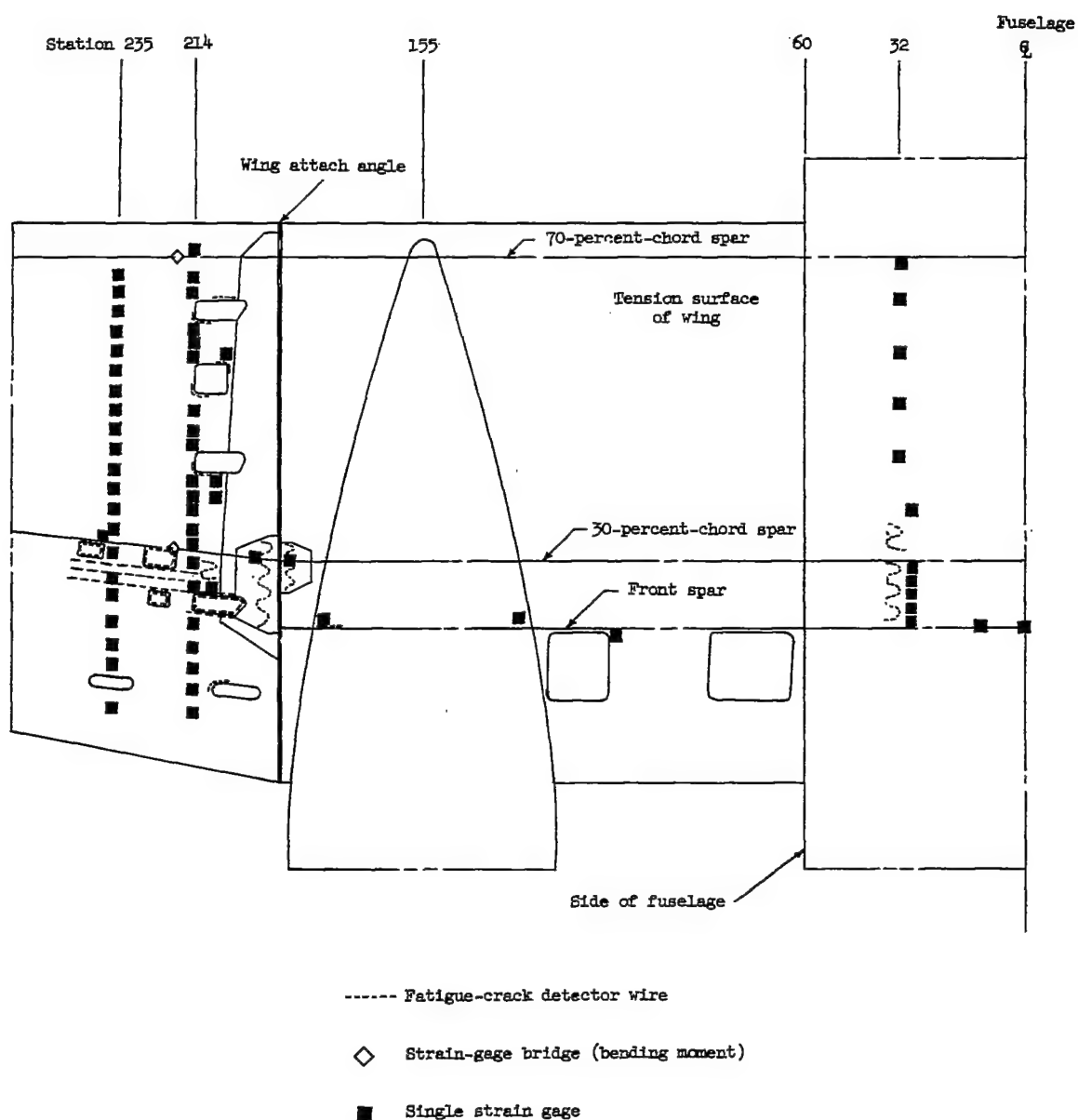
Figure 2.- Location of instrumentation on left wing. Installations are same on right wing.
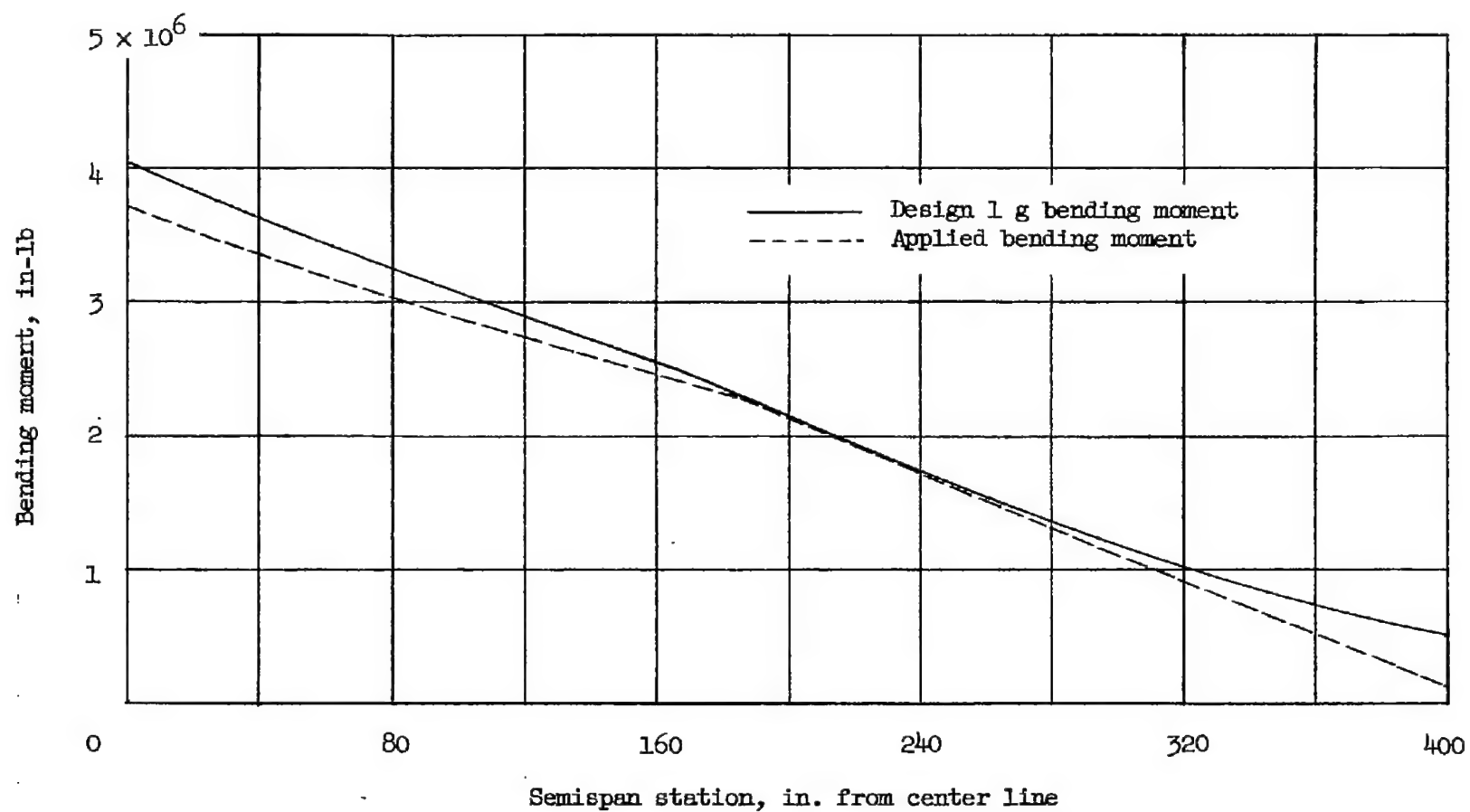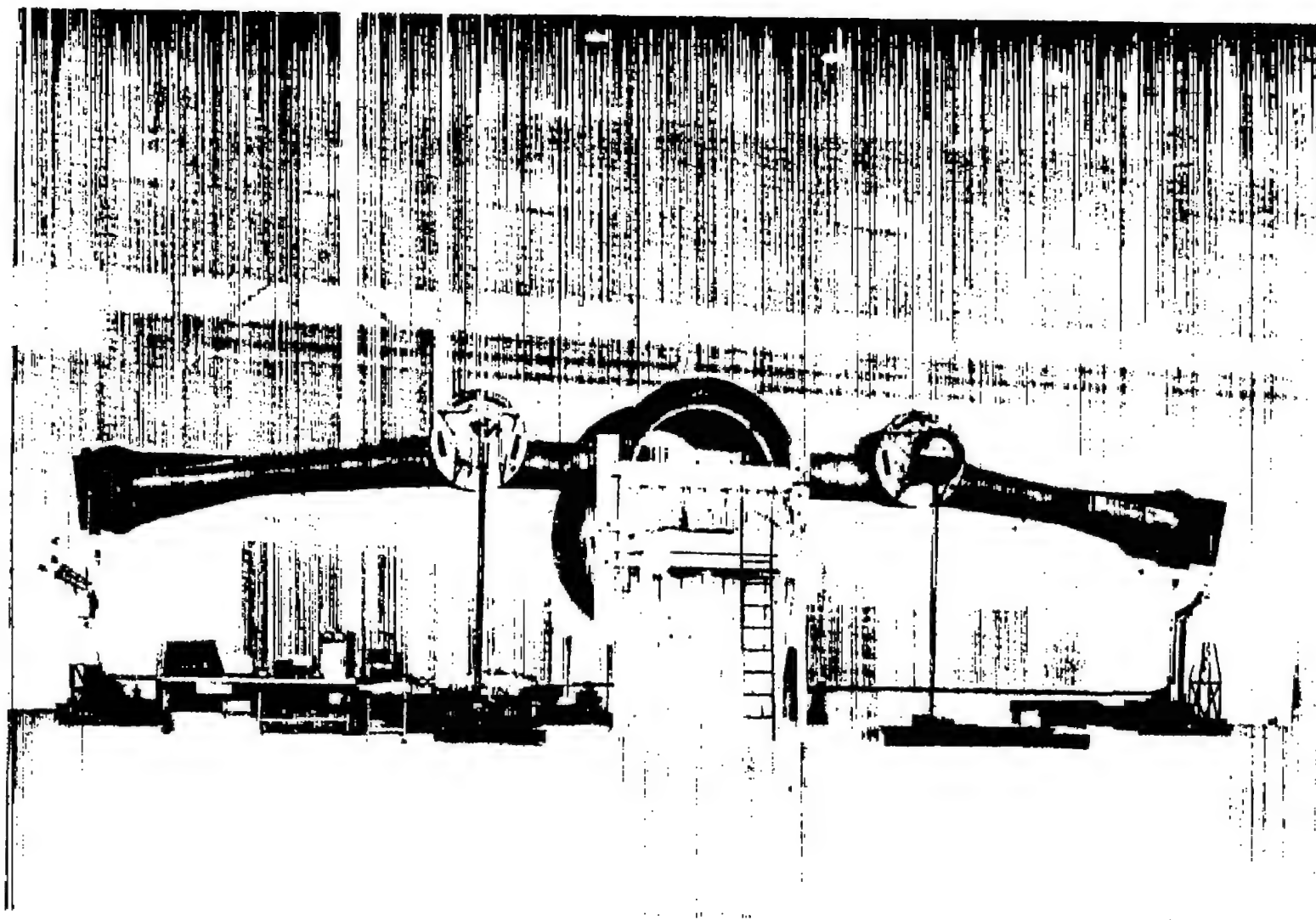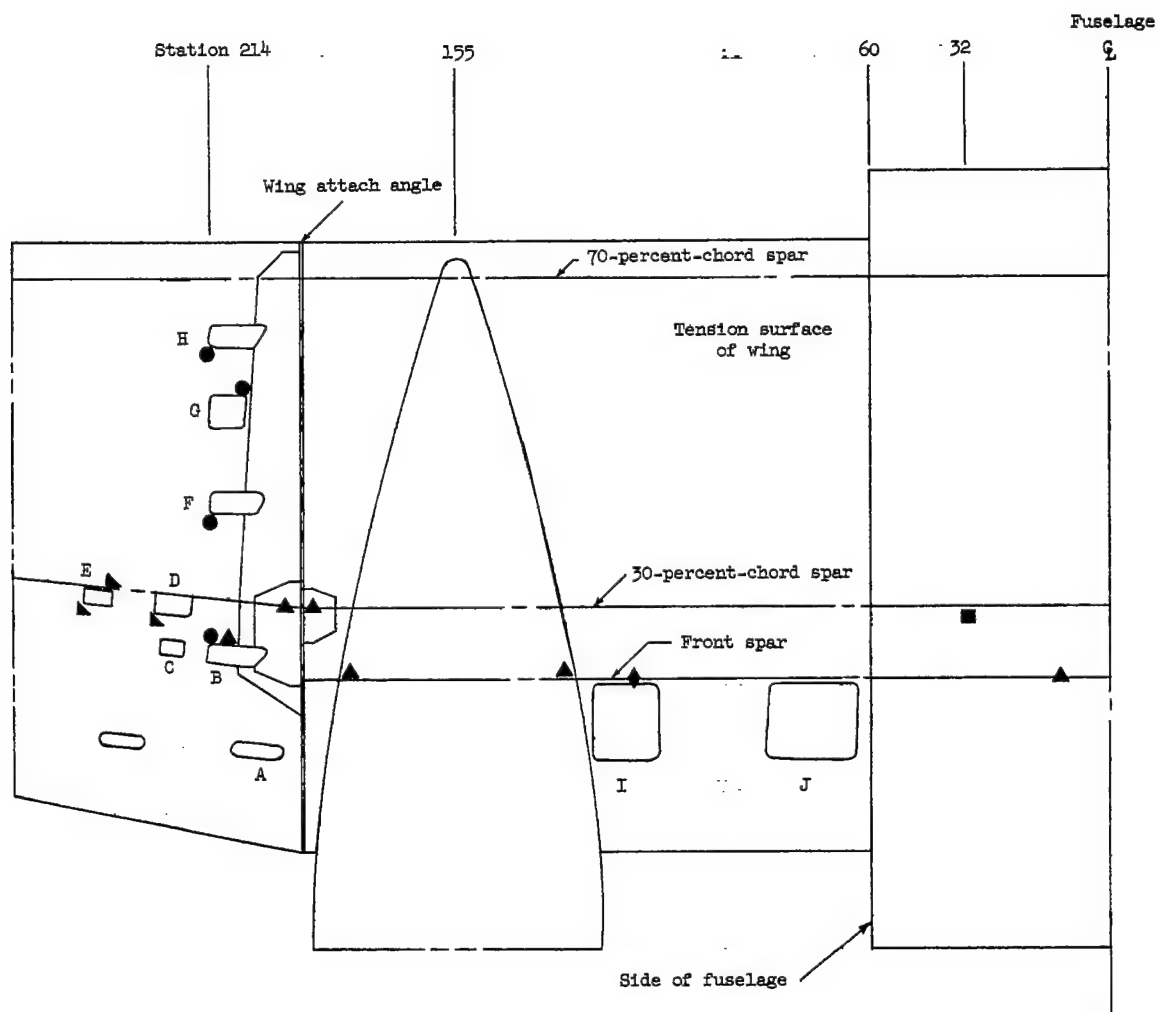
Figure 3.– Comparison of design and applied bending moments for the 1 g level-flight condition.

L-80028.1

Figure 4.- General view of wing mounted for test in fatigue machine.

Station 214   155   60   ·32   Fuselage
                                                                             ℄

Wing attach angle

70-percent-chord spar

H ●   Tension surface
                                              of wing
G ☐

F ●

E ▲   D   30-percent-chord spar
    ▲   ☐
      ● ▲   ■
  ☐   ◆   Front spar
C   B   ▲   ▲
                        ◆
                       ☐   ☐
▲   ▲
   A   I   J

Side of fuselage

●   Type I   Failures originating at the corners of inspection cutouts

■   Type II   Failures originating in riveted tension joints

◆   Type III   Failures originating in riveted shear joints

◣   Type IV   Failures originating in inspection cutout reinforcements

▲   Type V   Failures originating in miscellaneous discontinuities

Figure 5.- Locations and types of fatigue failures.
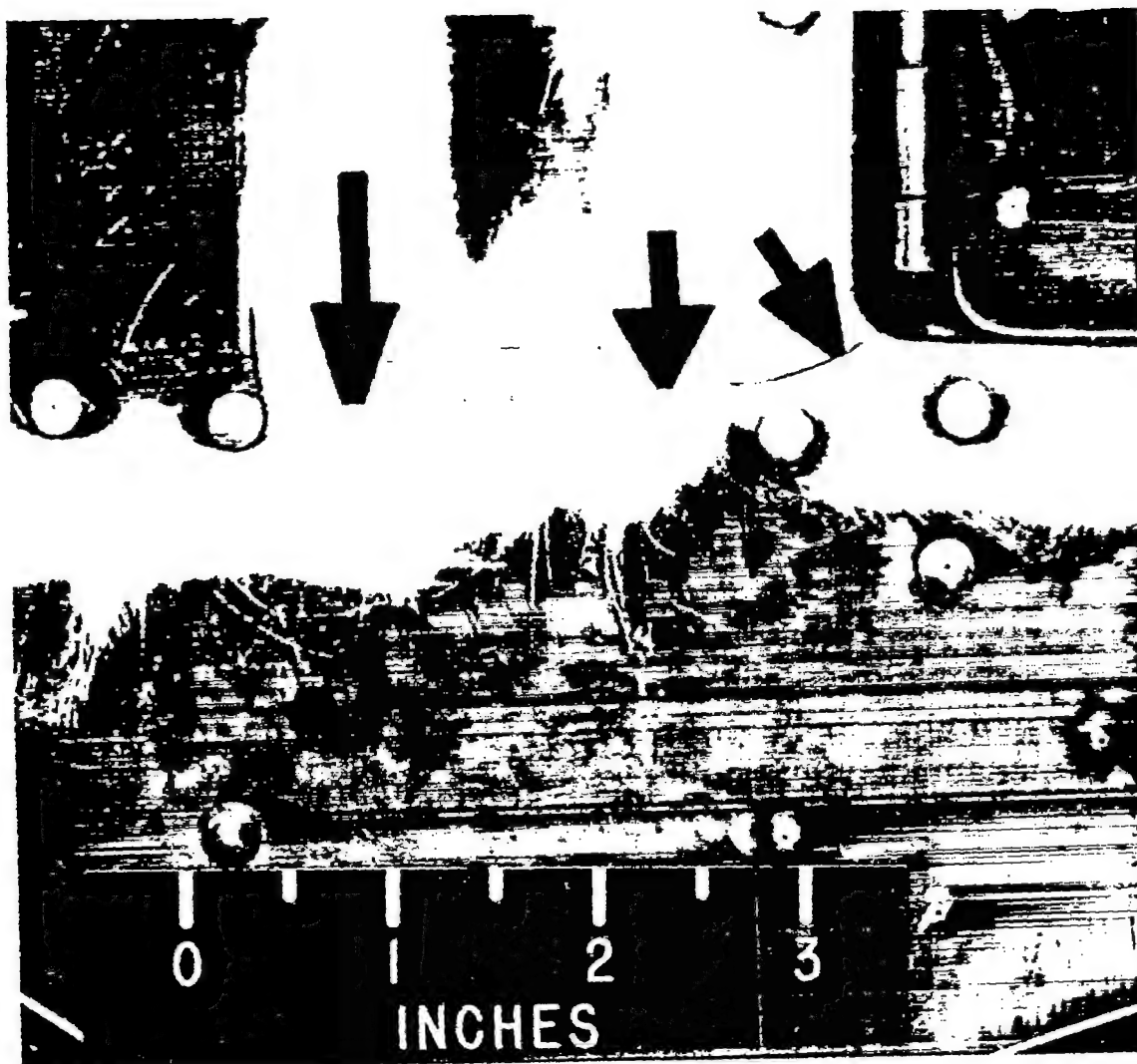
L-77922.4

(a) Type I failure at forward outboard corner of inspection cutout F.

Figure 6.- Illustrations of some of the types of failures.
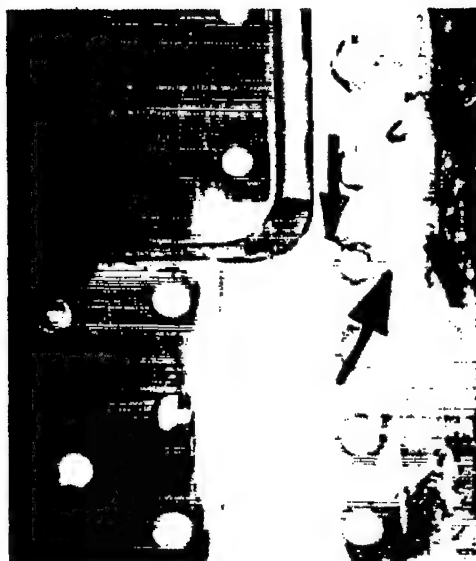
L-77923.1

(b) Type I failure at forward outboard corner of inspection cutout H.
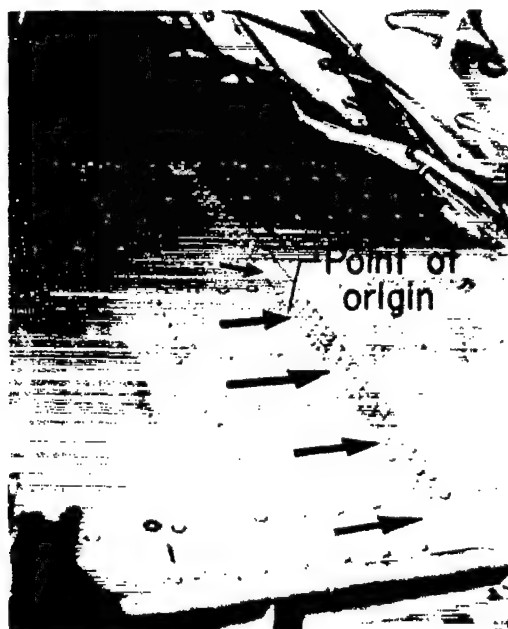
L-65799.2

(c) Type II failure in riveted tension joint.

Figure 6.- Continued.
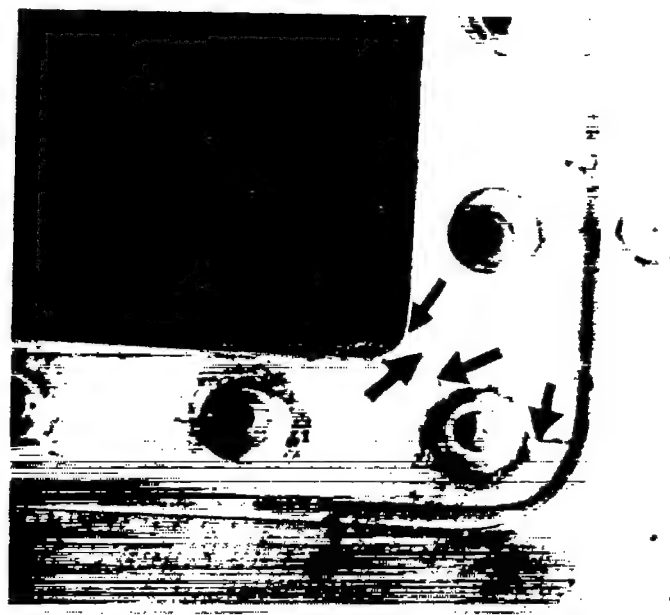
L-77924

(d) Type IV failure in reinforcing doubler plate at inspection cutout D.

L-67351.1
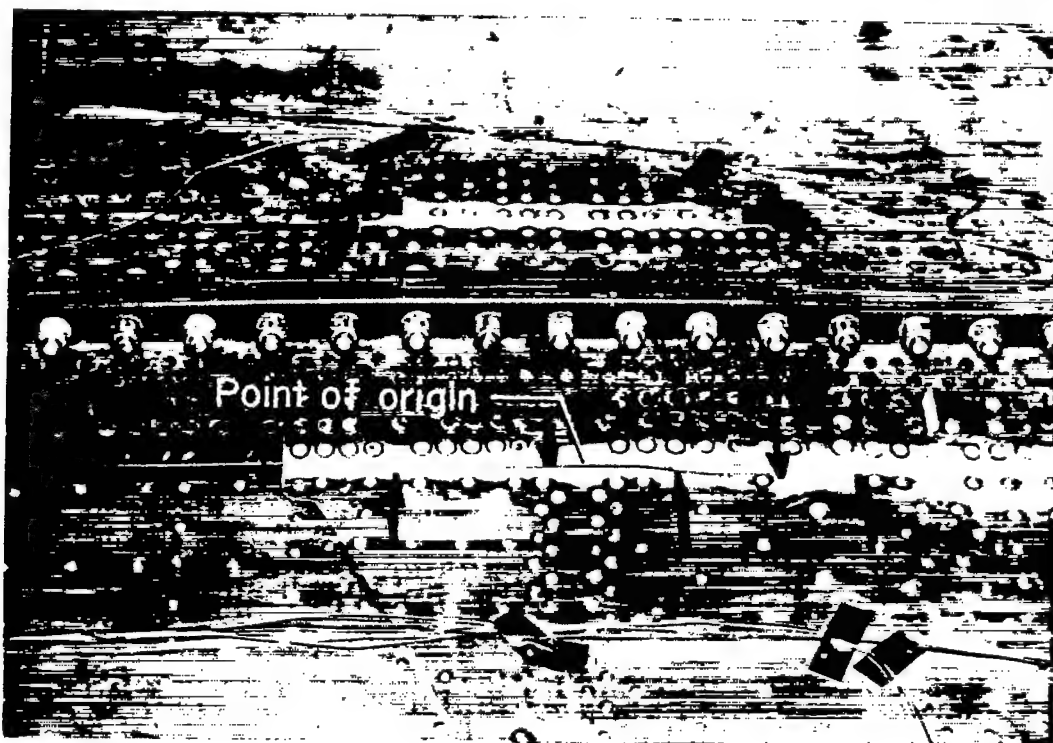
(e) Type V failure in joggle in external reinforcing doubler plate.

Figure 6.- Continued.
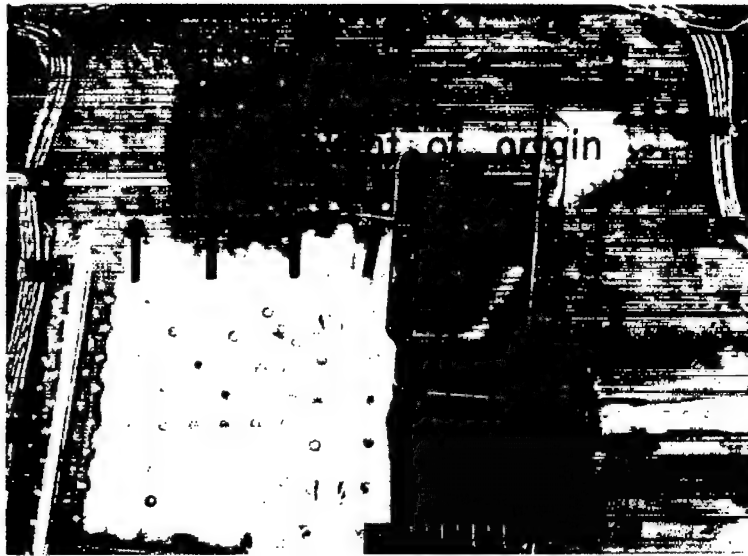
L-81785.2

(f) Type V failure at edge of external reinforcing doubler plate between
cutout B and 30-percent-chord spar.
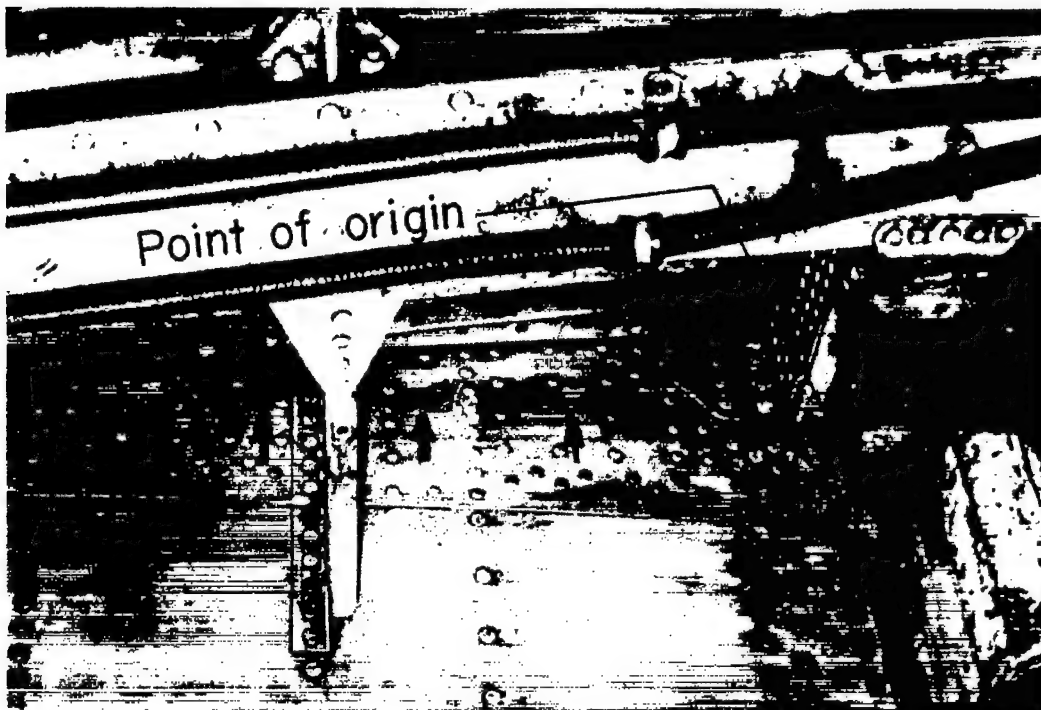
L-67783.1

(g) Type V failure inside engine nacelle.

Figure 6.- Concluded.

Section A-A

$3\frac{7}{16}$

Tension flange of
spar; area, 1.487 sq in.

Thickness, 0.064 in.

Thickness, 3/16 in.
Approximate area, 0.31 sq in.

.064

Rivet pitch for top two rows, $\frac{7}{8}$

Rivet pitch for bottom two rows, $\frac{11}{16}$

A

Typical
failure

All rivets
AN442AD-6

Shear web of spar

A
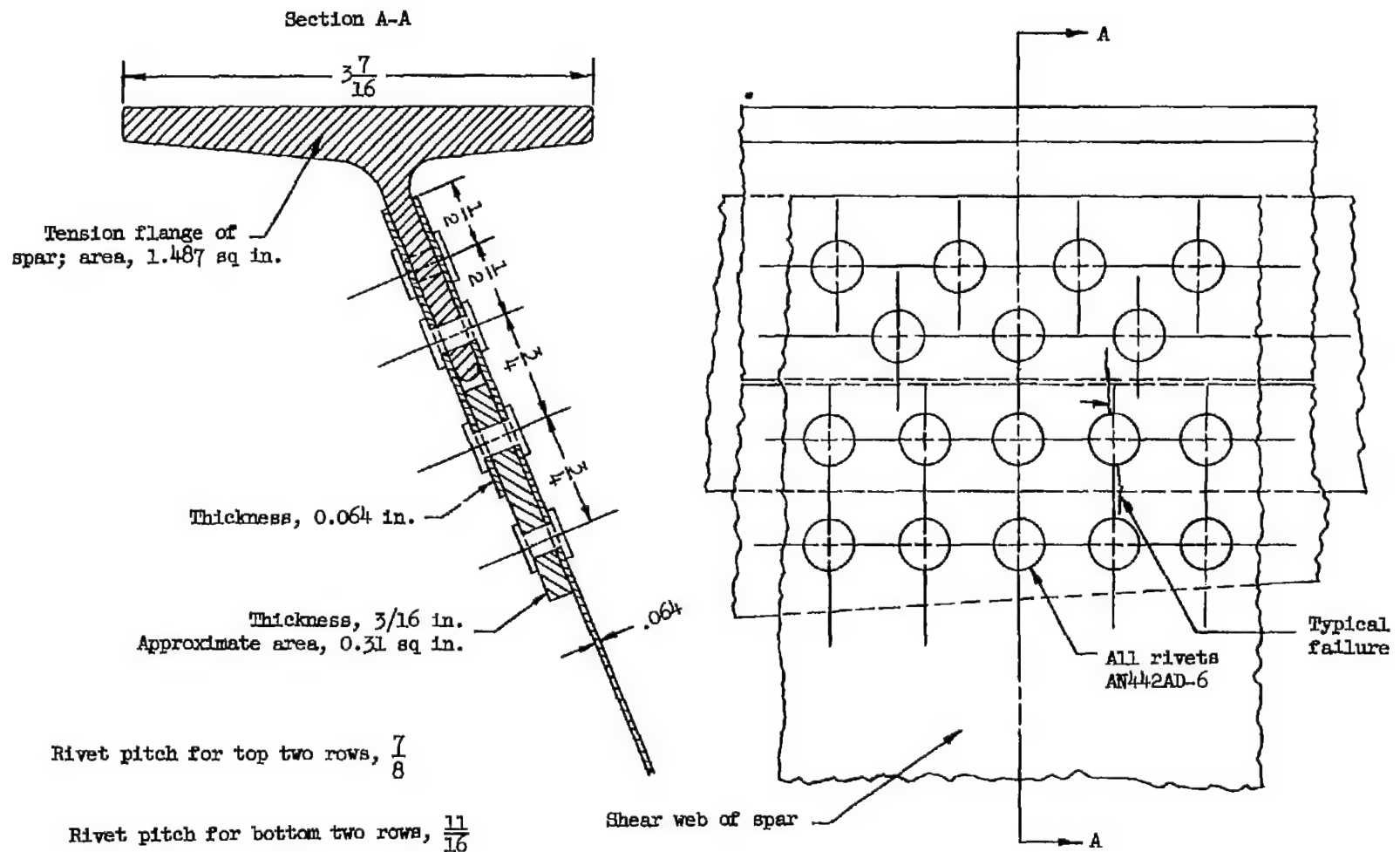
Figure 7.- Details of riveted shear joint at span station 120 in which
type III failures occurred.
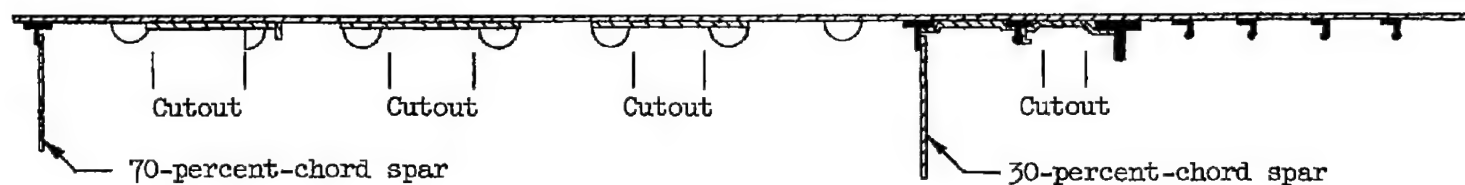
Cross section of tension surface at station 214
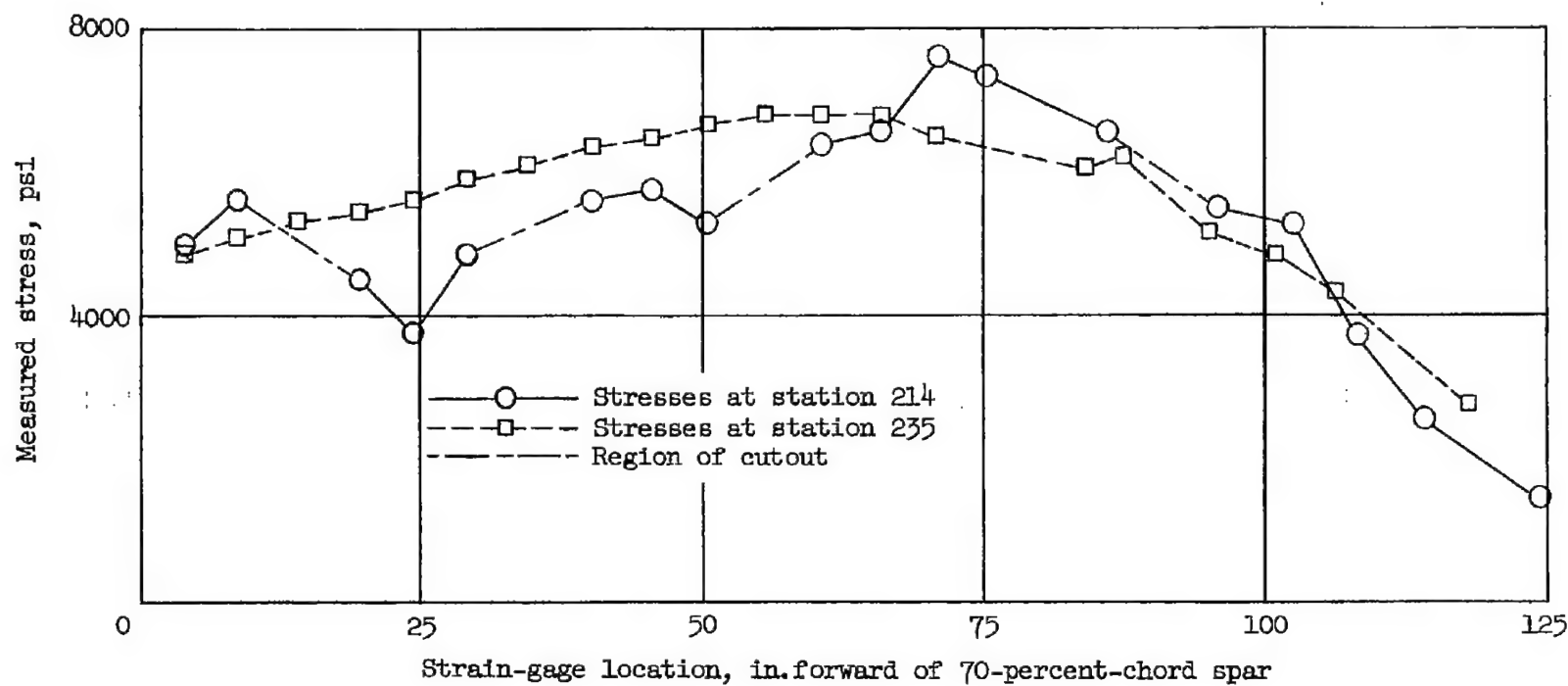
Figure 8.- Chordwise distribution of measured spanwise 1 g stresses.
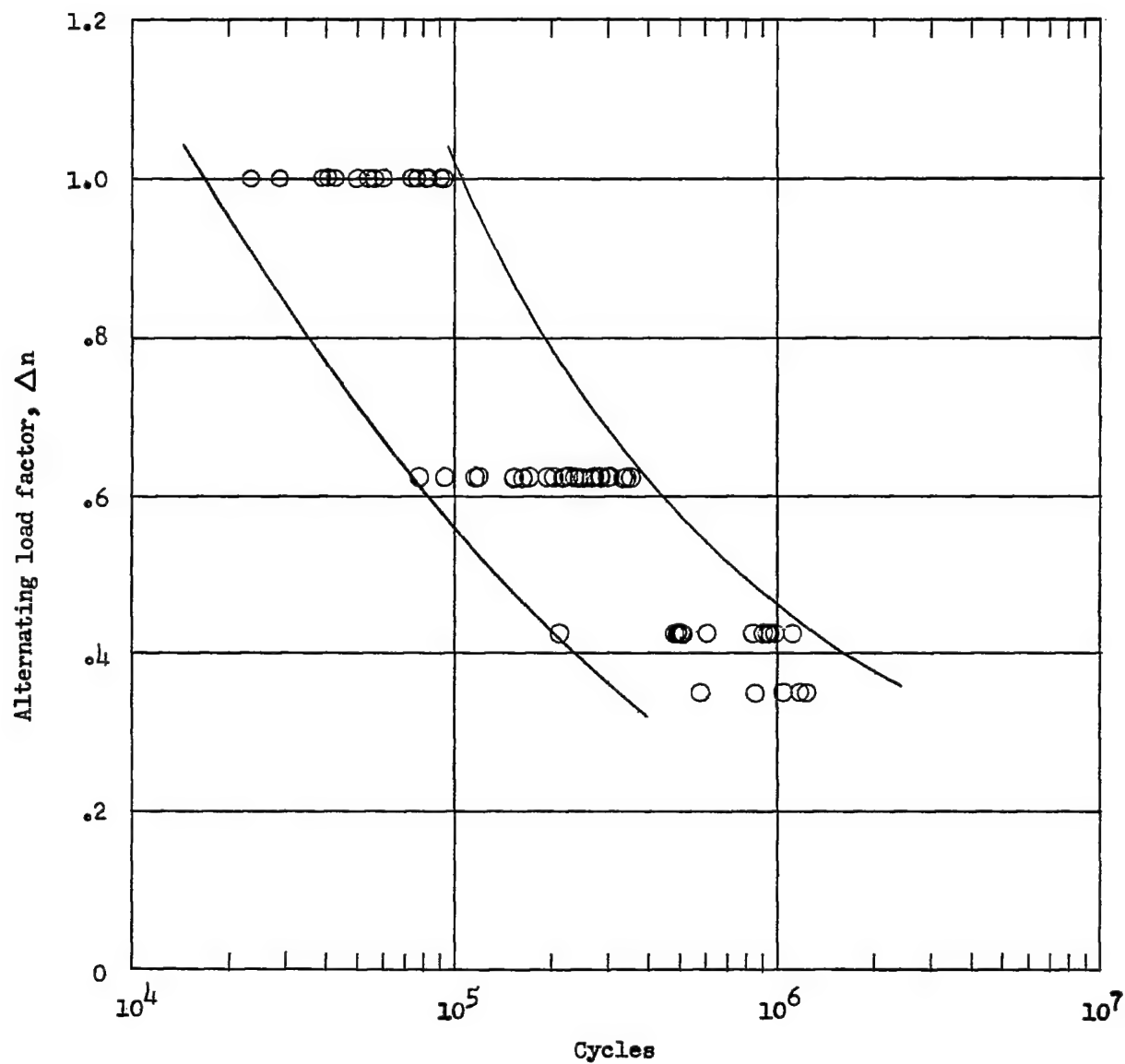
Figure 9.- Load-lifetime diagram for initial failure showing scatter band for 95-percent probability.
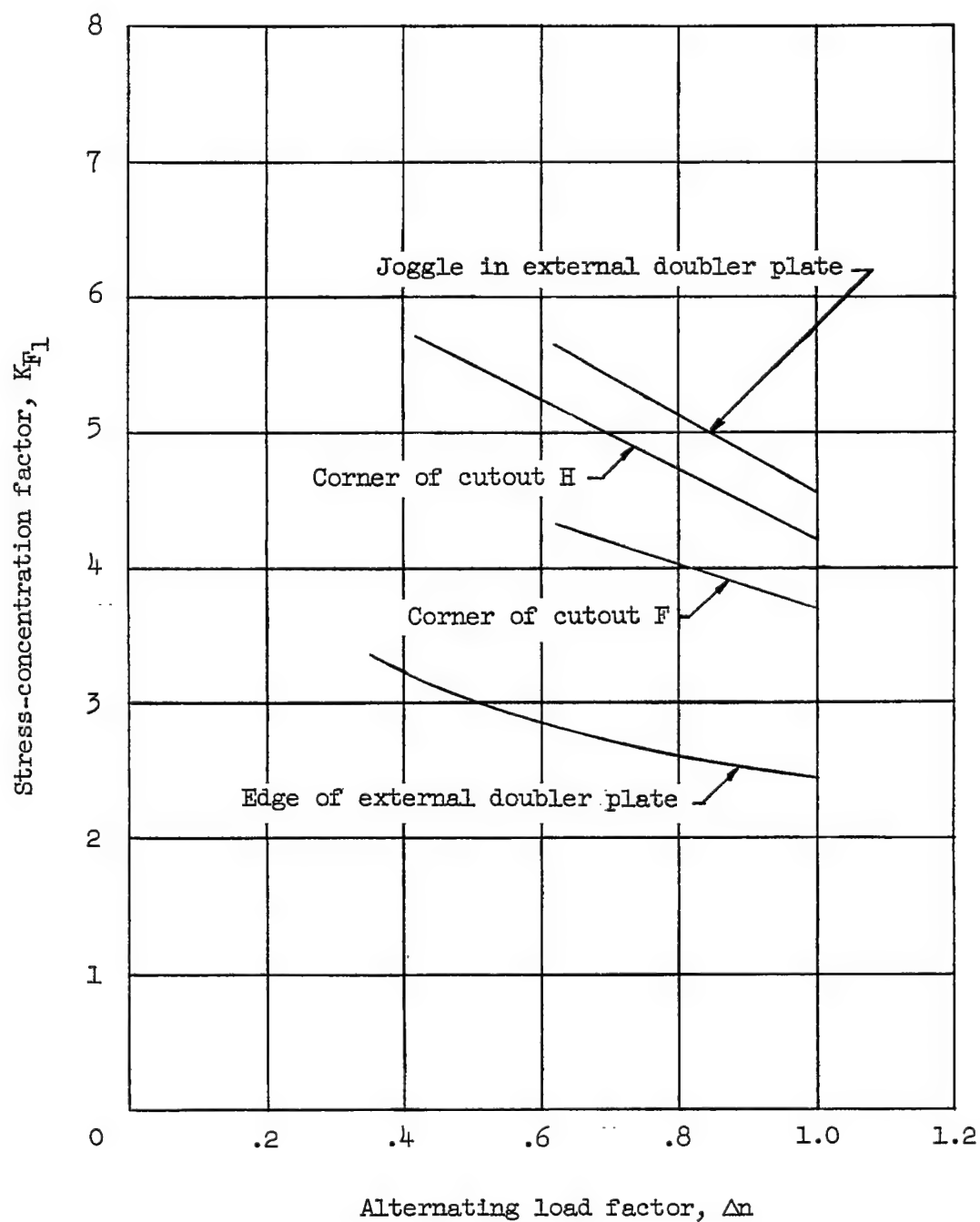
Figure 10.- Effect of load level on the stress-concentration factor.
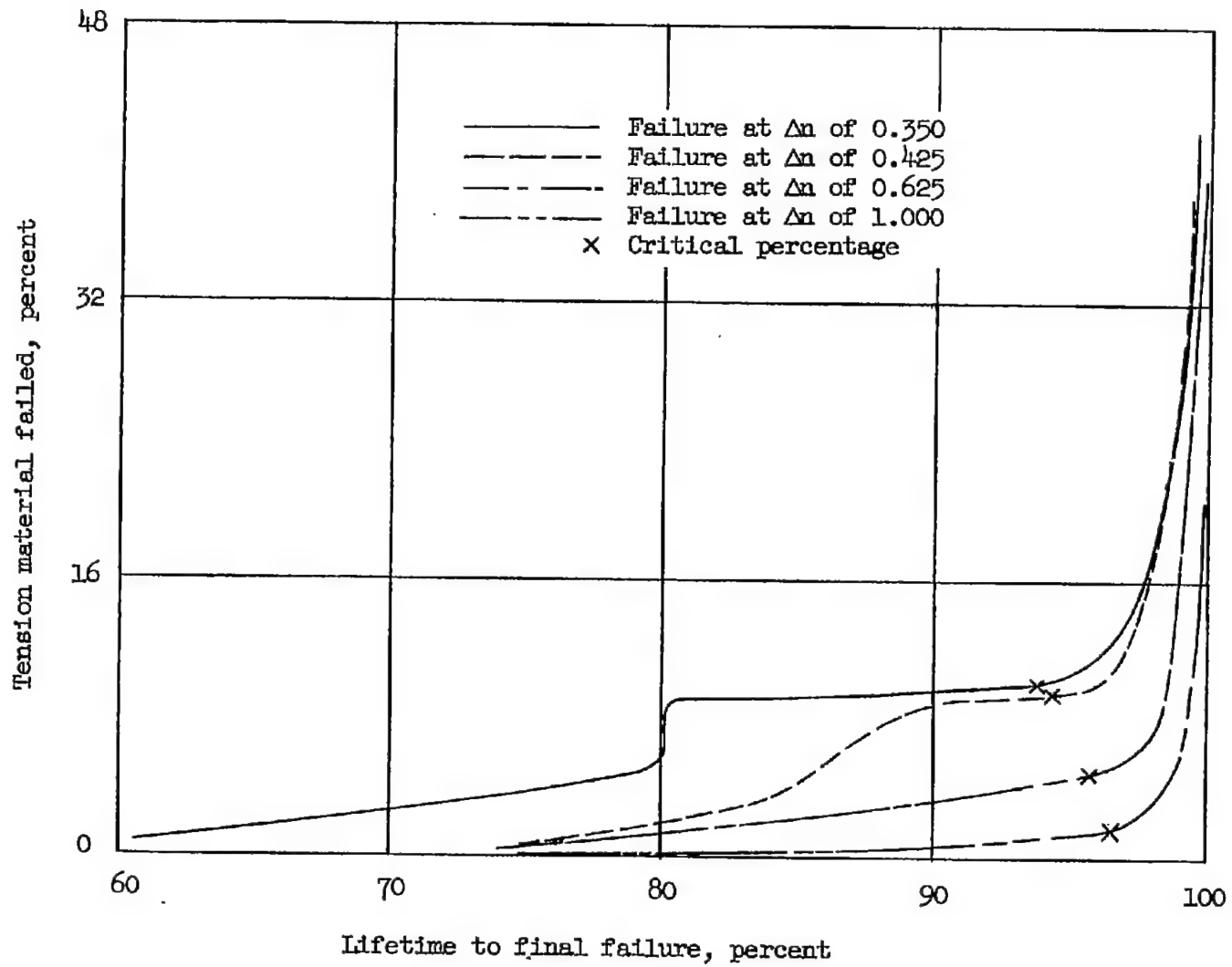
Figure 11.- Typical fatigue-crack propagation.
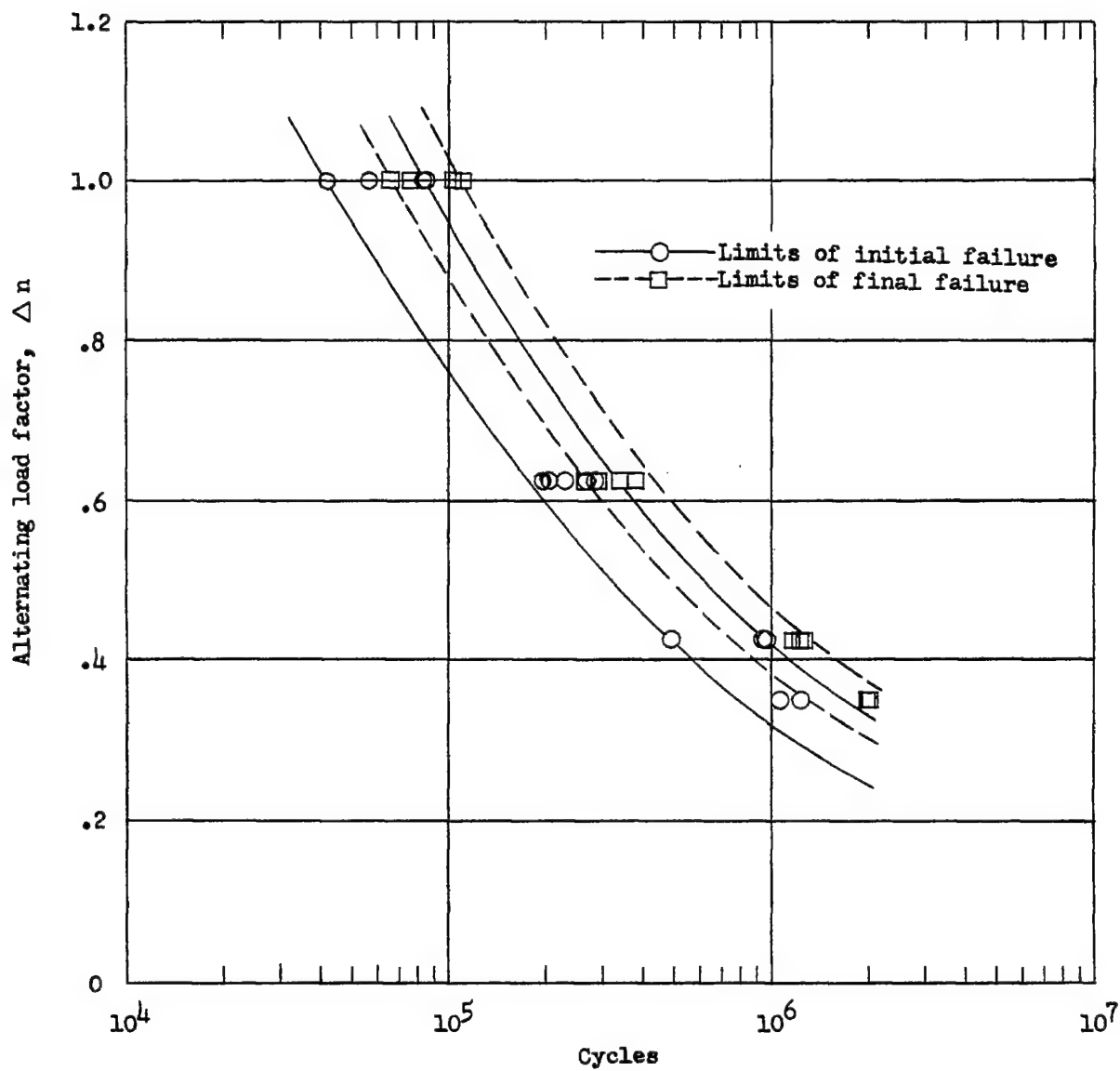
Figure 12.- Load-lifetime diagram for failures that grew past the
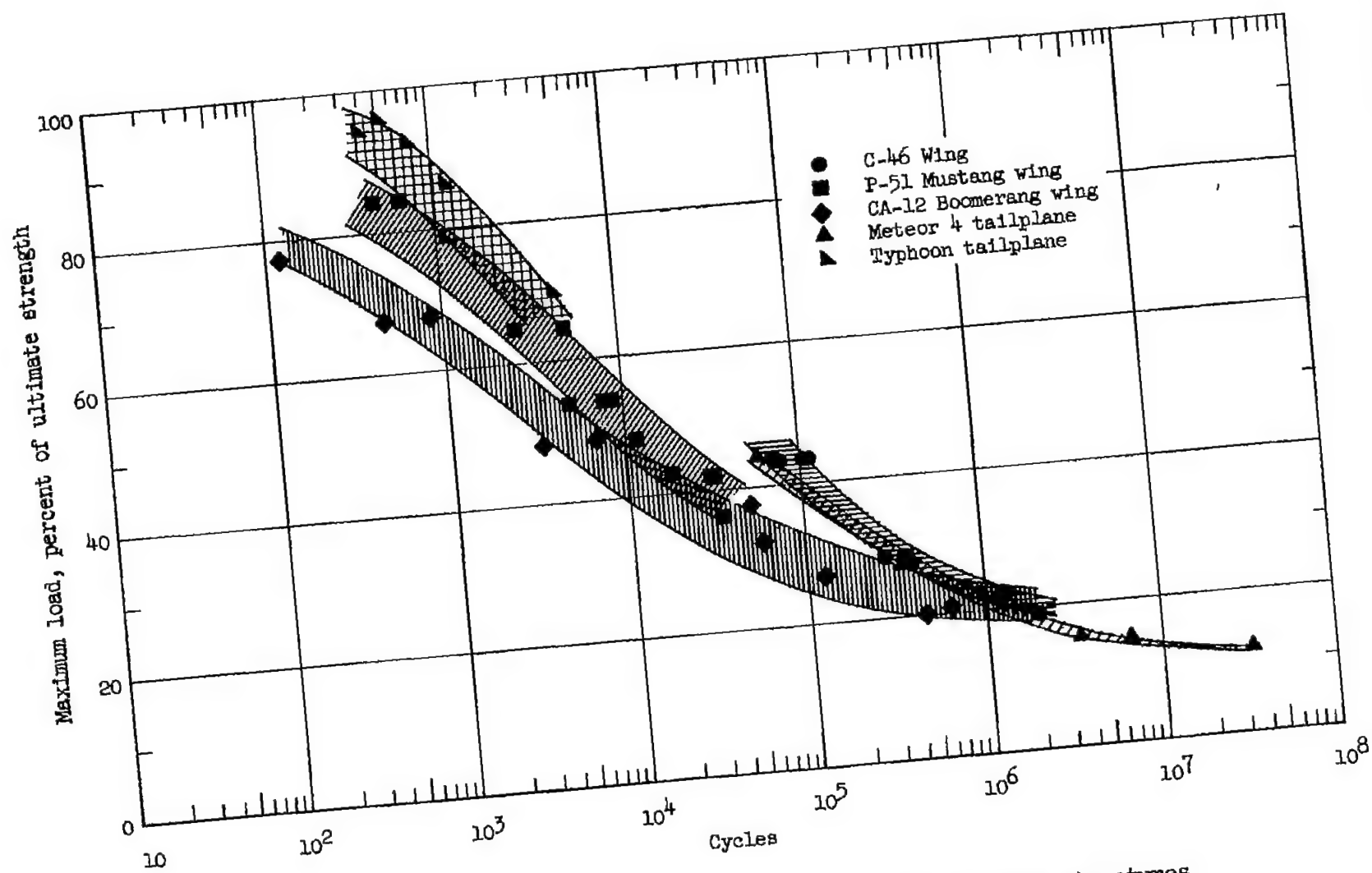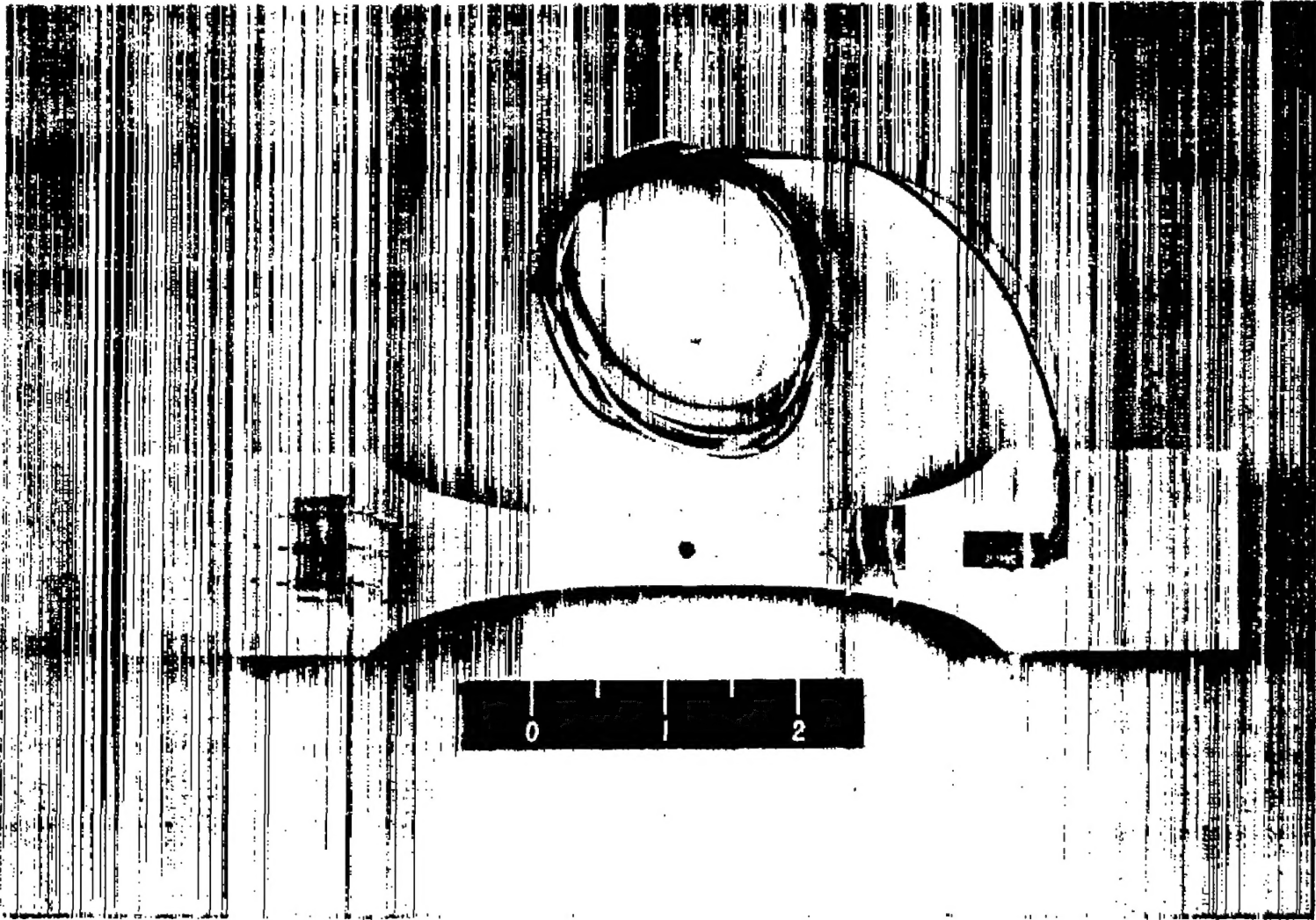critical point.

Figure 13.- Load-lifetime diagrams for several aircraft structures.

Figure 14.- Test specimen with a hole as a stress raiser. Fatigue-crack detector wire shown mounted close to hole.

L-76744
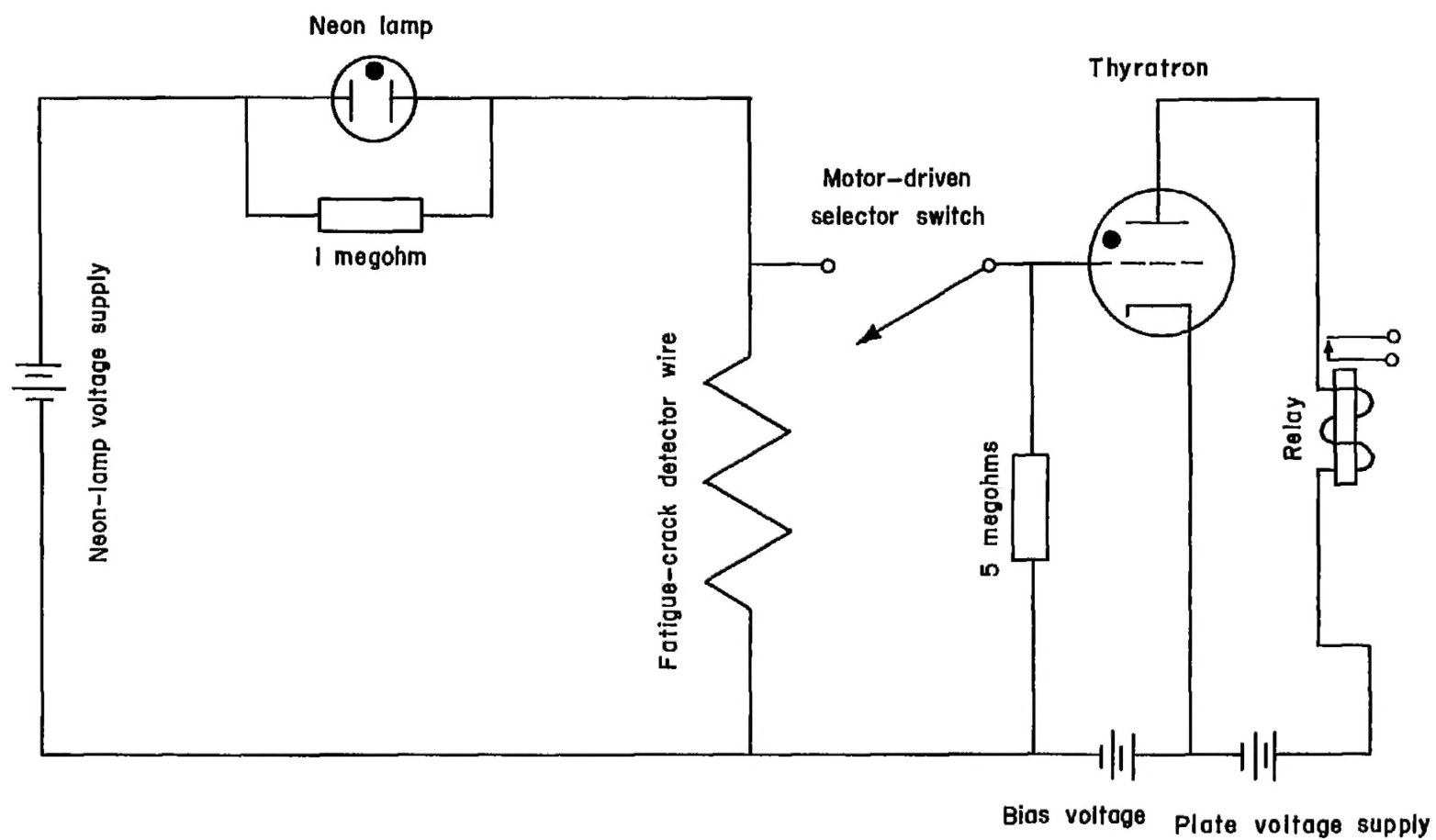
Figure 15.- Schematic diagram of a one-channel fatigue-crack-detector-
wire indicating circuit.

Fiber-glass
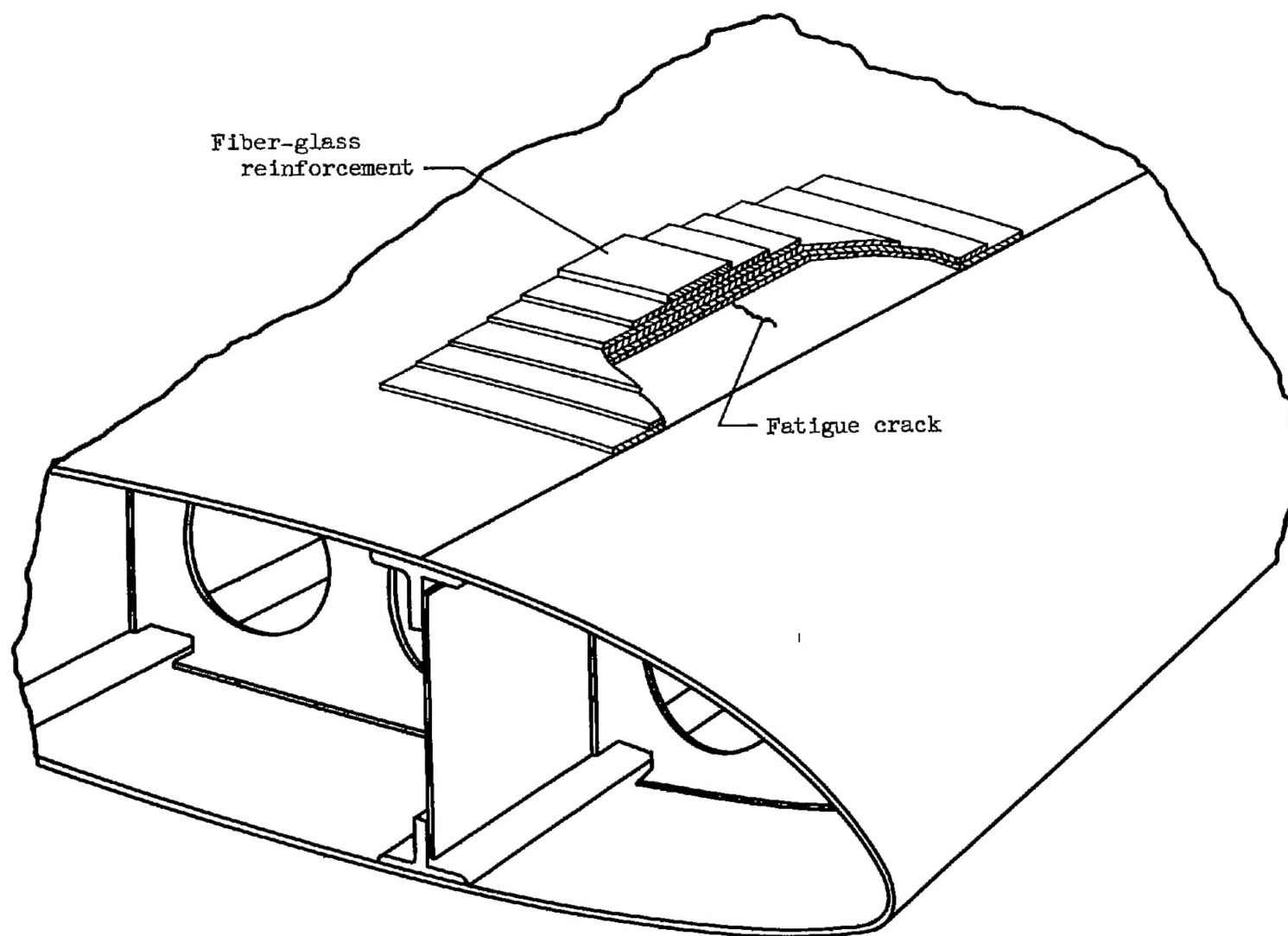reinforcement

Fatigue crack

Figure 16.- Typical arrangement of fiber-glass reinforcement.

L-71724

(a) Inside fuselage at span station 32.

L-83859.1

(b) Inside engine nacelle.

Figure 17.- Examples of fiber-glass repairs.